ChemComm

Stable metal-organic frameworks as host platform for catalysis and biomimetics

SCHOLARONE™
Manuscripts

ChemComm

Journal Name

ARTICLE

Stable metal-organic frameworks as host platform for catalysis and biomimetics

Jun-Sheng Qin,[†][a] Shuai Yuan,[†][a] Christina Lollar,[a] Jiandong Pang,[a] Ali Alsalme*[b] and Hong-Cai Zhou*[abc]

Recent years have witnessed the exploration and synthesis of an increasing number of metal–organic frameworks (MOFs). The utilization of stable MOFs as a platform for catalysis and biomimetics is discussed. This Feature Article will provide insights on the rational design and synthesis of three types of stable MOF catalysts on the basis of structural features of MOFs, that is, i) MOF catalysts with catalytic sites on metal nodes, ii) MOF catalysts with catalytic sites immobilized in organic struts, and iii) MOF catalysts with catalytic centres encapsulated in the pores. Then, MOFs used in biomimetics including biomimetic mineralization, biosensor and biomimetic replication are introduced. Finally, a discussion on the challenges that must be addressed for successful implementation of MOFs in catalysis and biomimetics is presented.

1. Introduction

As a new emerging class of crystalline porous materials, metal-organic frameworks (MOFs, also known as porous coordination polymers (PCPs) or porous coordination networks (PCNs)) possessing fascinating structures have attracted increasing attention mainly driven by their diverse applications, including gas sorption and separation,[1, 2] luminescence,[3] catalysis,[4, 5] and so on.[6-8] The assembly of metal ions and organic linkers by means of coordination bonds affords MOFs with cavities (cages or channels). The modular nature of MOFs derived from the rational combination of various metal nodes and organic linkers imparts adjustable porosity, tunable functionality and designable topology. One of the representative examples of this is the construction of MTV-MOFs (multivariate MOFs) by Yaghi *et al.*, in which up to eight linear linkers with the same length but bearing distinct functional groups were introduced into one framework.[9] The availability of diverse building blocks composed of metals and organic linkers makes it possible to construct MOFs with tunable pore sizes, shapes as well as environments,[10] meanwhile, MOFs represent a feasible platform for post-synthetic modifications.[11] Furthermore, mixed-linker strategy provides more opportunity to construct multifunctional MOFs.[12, 13]

The structural diversity and tunability of MOFs imparts all MOF components (nodes, linkers and pores) to be modified with various catalytic sites into a single material.[14, 15]

Generally, MOFs as catalysts possess the following advantages over the traditional porous materials (such as, zeolites, clays or mesoporous silica): i) uniformly dispersed catalytic active sites on the pore surfaces at the molecular level that favours for the mechanism study, ii) hydrophilic and hydrophobic pore environments that are suitable for the recognition and transportation of reactants and products, and iii) a collaborative microenvironment that is favourable for playing a positive role in synergistic catalysis. However, the chemical stability of MOFs limits their separation and recovery as solid heterogeneous catalysts.[16] Therefore, researchers in recent years have devoted great efforts to developing stable MOF catalysts,[17] which were composed of either carboxylate linkers with high-oxidation-state metal species[18, 19] or nitrogen containing ligands with divalent metals.[20]
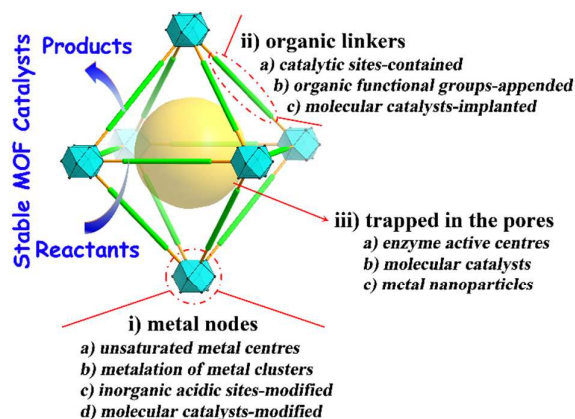
Scheme 1. Classification of different positions in MOF materials where catalytic reactions can take place. The metal nodes and organic linkers are indicated with cyan polyhedra and green rods, whereas the pore is indicated in yellow sphere.

a. Department of Chemistry, Texas A&M University, College Station, Texas 77843-3255, United States.
b. Chemistry Department, College of Science, King Saud University, Riyadh 11451, Saudi Arabia.
c. Department of Materials Science and Engineering, Texas A&M University, College Station, Texas 77843-3003, United States.
† Jun-Sheng Qin and Shuai Yuan contributed equally.

In this Feature Article, we focus on the recent progress on MOFs for heterogeneous catalysis and biomimetic study, especially for stable Cr(III), Al(III), Zr(IV) and Hf(IV)-based MOFs, and zeolite-like MOFs (also known as zeolitic imidazolate frameworks, ZIFs). According to their structural features (metal nodes, organic linkers and pores), three kinds of MOF catalysts were described in the article (Scheme 1), that is, i) MOF catalysts with catalytic sites on metal nodes, ii) MOF catalysts with catalytic sites immobilized in organic struts, and iii) MOF catalysts with catalytic centres encapsulated in the pores. As for the first type, catalytic sites on metal nodes, it can be divided into four subgroups: a) coordinatively unsaturated metal centres as catalytic sites, b) the metalation of metal clusters with other active transition metals, c) the modification of metal clusters with inorganic acidic sites, and d) the modification of metal clusters with molecular catalysts. Then, three subgroups related to the second type will be introduced, namely, a) organic linkers with catalytic sites as struts, b) the organic functional groups appended to the organic linkers, and c) the rational modification of organic linkers with molecular catalysts. As for the third type, the catalytic centres (for instance, enzyme active centres, molecular catalysts and metal nanoparticles) can be encapsulated the pores of MOFs, which are freely contacted with the incoming reactant molecules and thereby to realize efficient catalysis. Generally, the catalytic sites employed to modify the MOF materials in the literature have been proved to possess certain catalytic activity. The catalytic sites can be placed in the well-defined positions of MOFs through either rational design of metal nodes, organic linkers and environments of pores, or postsynthetic modification. Therefore, we would like to introduce the advances made towards these three types of stable MOF catalysts that would be helpful for gaining a better understanding on the relationship between the synthetic chemistry and catalytic applications. The recent developments, discussions and challenges related to the introduction of catalytic sites and catalysis performance of MOF catalysts will be demonstrated in this article. Finally, stable MOFs used for biomimetic study are also be introduced and discussed.

2. MOF catalysts with catalytic sites on metal nodes

The coordination sites of metal nodes, either coordinatively vacant or coordinating to volatile solvent molecules (for example, water and DMF) resulting from the constrain between the directionality of rigid organic linkers and the coordination geometry of metal nodes, can be easily removed/replaced without decomposition of their original framework structures. The presence of open metal centres of metal nodes in MOFs makes it be used as catalysts. However, the study of MOF catalysts with open metal centres as catalytic sites is still in its infancy. Various methods have been developed to incorporate active species (for instance, other active transition metals, inorganic acidic sites and molecular

Table 1 The summary of MOF catalysts with catalytic sites on metal nodes

MOF	Active site	Reaction	Ref.
MIL-101	Cr(III)	benzaldehyde cyanosilylation	22
MIL-101	Cr(III)	sulfoxidation of aryl sulfides	23
MIL-101	Cr(III)	oxidation of tetralin	24
MIL-101	Cr(III)	oxidation of alkenes	25
MIL-101	Cr(III)	styrene oxidation	26
MIL-101	Cr(III)	CO_2 cycloaddition	27
Hf-NU-1000	Hf(IV)	CO_2 cycloaddition	28
Hf-NU-1000	Hf(IV)	oxidation of styrene	29
NU-1000	Zr(IV)	hydrolysis of methyl paraoxon	30
Zr-AzoBDC	Zr(IV)	amidation of benzoic acids	31
UiO-66(NH₂)	Zr(IV)	cross-aldol condensation	32
UiO-66(X)	Zr(IV)	cyclization of citronellal	33
UiO-66-NH₂	Zr(IV)	phosphate-ester hydrolysis	34,35
Ti-UiO-66	Ti(IV)	CO_2 reduction	37
Ti-UiO-66	Ti(IV)	cyclohexene oxidation	38
Al-NU-1000	Al(III)	ethanol dehydration	41
CoS-AIM	Co(II)	*m*-nitrophenol hydrogenation	42
Ni-AIM	Ni(II)	ethylene hydrogenation	43
NiS-AIM	Ni(II)	H_2 generation	44
Mo-SIM	Mo(VI)	cyclohexene epoxidation	45
Nb-AIM	Nb(V)	alkene epoxidation	46
Co-SIM+NU-1000, Co-AIM+NU-1000	Co(II)	oxidative dehydrogenation of propane, water oxidation	47,48
Hf-NU-1000-ZrBn	Zr(IV)	olefin polymerization	49
Ni-AIM	Ni(II)	hydrogenation of light olefins	50
Cu-NU-1000	Cu(II)	methane oxidation	51
Co−Al-NU-1000	Co(II), Al(III)	alcohol oxidation	52
VUiO-66	V(V)	oxidative dehydrogenation of cyclohexene	53
Ni-AIM+UiO-66	Ni(II)	ethylene hydrogenation	54
PCN-800(In)	In(III)	acetaldehyde cyclotrimerization	55
UiO-CoCl or UiO-FeBr	Co(II) or Fe(III)	borylation and silylation of benzylic C–H bonds, hydrogenation and hydroboration of alkenes, ketones, sp³ C–H amination	56

ARTICLE

Zr-MTBC-CoH	Co(II)	hydrogenation of alkenes, imines, carbonyls, and heterocycles	57
CeH-BTC	Ce(III)	hydroboration of pyridine and alkenes and hydrophosphination of alkenes	58
ZrMe-BTC	Zr(IV)	ethylene polymerization	59
MOF-808-2.5SO$_4$	−SO$_4$ and Zr(IV)	Friedel−Crafts acylation, esterification, and isomerization	60
MIL-101(Cr)-SO$_3$H	−SO$_3$H and Cr(III)	hydrogenation of imines	61
PO$_4$/NU-1000	−PO$_4$ and Zr(IV)	glucose transformation	62
MIL-101-Cr-SO$_3$H·Al(III)	−SO$_3$H, Cr(III) and Al(III)	benzylation of aromatic hydrocarbons	64
(1,1'-ferrocenediyl-dimethylsilane)$_{0.25}$@MIL-53(Al)	1,1'-ferrocenediyl-dimethylsilane	benzene oxidation	65
NU-1000-(bpy)Ni^{II}	−(bpy)Ni^{II}	ethylene dimerization	66
Ir-pincer modified NU-1000	Ir-pincer	hydrogenation of alkene	67
[Fe$_3$(μ$_3$-O)(bdc)$_3$]$_4$[Co$_2$(na)$_4$(L^T)$_2$]$_3$	[Co$_2$(na)$_4$(L^T)$_2$]	oxygen evolution reaction	68
BODIPY/NU-1000	BODIPY	detoxification of sulfur mustard	69

catalysts) into stable MOFs in order to obtain MOF catalysts with high performance (Table 1).

2.1. Coordinatively unsaturated metal centres as catalytic sites

To create unsaturated metal centres into the metal nodes of MOFs is a simple way to encapsulate Lewis or Brønsted acid sites, which can be employed directly as heterogeneous catalysts. MIL-101(Cr) (Cr$_3$X(H$_2$O)$_2$O(1,4-bdc)$_3$; X = F, OH; bdc = benzene-1,4-dicarboxylate), initially published by Férey et al.,[21] is an ideal stable MOF for applications in heterogeneous catalysis because of the following reasons. On the one hand, its pore sizes (29 to 34 Å) and pore windows (pentagonal window with a free opening of ~12 Å and hexagonal window with a free aperture of ~14.5 Å × 16 Å) are large enough to give access for the diffusion of reactants and the release of product molecules. On the other hand, the water molecules coordinated to chromium centres can be easily removed in vacuum and at elevated temperature, leaving open chromium sites accessible for potential reactants. In this context, MIL-101(Cr) was tested as heterogeneous catalysts for aldehydes cyanosilylation,[22] sulfides and hydrocarbons oxidation,[23-26] and CO$_2$ cycloaddition.[27]

Hupp and Farha et al. reported a permanently porous Hf$_6$ cluster-based MOF, Hf-NU-1000. Due to the high density of Lewis acidic sites present within the framework, Hf-NU-1000 demonstrates high excellent catalytic performance for the quantitative chemical fixation of CO$_2$ into five-membered cyclic carbonates under ambient conditions.[28] Besides, Hf-NU-1000 also exhibits the regioselectivity and enantioretentivity for the formation of 1,2-bifuctionalized systems via solvolytic nucleophilic ring opening. In addition, Hf-NU-1000 can be recycled and reused for multiple successive runs without considerable loss of activity or structural deterioration. In light of this, they envisioned that a robust MOF composed of Fe−porphyrin-based struts and catalytically active Hf$_6$ nodes would generate a catalyst capable of performing tandem epoxidation and subsequent epoxide opening. As a result, they prepared a Fe−porphyrin variant of Hf-NU-1000, namely Hf-2, and a postsynthetically-metalated structure, Fe@Hf-2, which contains Fe in the porphyrin struts as well as two additional Fe atoms on the Hf$_6$ nodes.[29] Hf-2 demonstrates catalytic efficacy in the tandem oxidation and functionalization of styrene utilizing O$_2$ as a terminal oxidant. Significantly, the unusual regioselective transformation occurs as a Fe-decorated Hf$_6$ node and the Fe−porphyrin strut work in concert in Fe@Hf-2. This work presents an example of concurrent orthogonal tandem catalysis. Meanwhile, nano-sized NU-1000 was also used as the catalyst for the degradation of a nerve agent simulant (methyl paraoxon) as a function of NU-1000 crystallite size.[30]

An azobenzene-containing Zr-MOF with UiO topology, termed Zr-AzoBDC (AzoBDC = azobenzene-4,4'-dicarboxylate), was prepared by Truong and coworkers.[31] Zr-AzoBDC, as a heterogeneous catalyst for the direct amidation of benzoic acids in tetrahydrofuran, exhibited exceptional catalytic activity under mild conditions and can be reused to new reactions without degradation in catalytic activity. In addition, Zr-AzoBDC can be widely used to a variety of substituted carboxylic acid and amine derivatives for the synthesis of bioactive amide compounds.

Besides, the catalytic activity of MOFs with coordinatively unsaturated sites can be strongly improved by using functionalized linkers. In UiO-66, each Zr$_6$O$_4$(OH)$_4$ octahedron is surrounded by maximally 12 terephthalate linkers, leading to large octahedral and small tetrahedral cages. Speybroeck and Vos employed a series of 1,4-bdc derivatives (1,4-bdc-X; X = H, NH$_2$, CH$_3$, OCH$_3$, F, Cl, Br, NO$_2$) to synthesize UiO-66 analogues.[32, 33] To test the effect of the substituents, the cyclization of citronellal to isopulegol isomers was chosen, in which the selectivity of product depends strongly on the Lewis acidity of the active site. The catalytic results suggest that the substituents not only alter the Lewis acidic activities but induce additional stabilizing or destabilizing effects on the reactants derived from their electronic properties. Hupp and Farha utilized 1,4-bdc derivatives to synthesize UiO-66-NO$_2$, UiO-66-(OH)$_2$ and UiO-66-NH$_2$, which were used as catalysts for phosphate-ester hydrolysis.[34, 35] Among them, UiO-66-NH$_2$ showed a great increase in hydrolysis rate over the parent UiO-66 and other UiO-66 derivatives.[34] A similar phenomenon occurred in UiO-67 species. The authors proposed that the role of the amino group is to act as a proton-transfer agent during the catalytic cycle.

2.2. The metalation of metal clusters with other active transition metals

Compared with high-oxidation-state metal species, low-valent transition metals exhibit excellent catalytic activities. However, the low-valent transition metal-based MOFs are usually sensitive to the ambient moisture, aqueous solutions, and acid and base media, which hampers their practical applications. In this context, efforts have been made to functionalizing the metal clusters of Zr-MOFs with other transition metal centres. In fact, bimetallic MOFs can be realized by post-synthetic metal exchange or metalation of Zr_6 cluster.

Cohen *et al.* synthesized a titanium-containing analogue of UiO-66, namely Ti-UiO-66, by post-synthetic metal exchange of Zr(IV) with Ti(IV),[36] which was further revealed to exhibit enabled photocatalytic CO_2 reduction to HCOOH under visible light irradiation with the aid of 1-benzyl-1,4-dihydronicotinamide (BNAH) and triethanolamine (TEOA).[37] A comparative study of the Ti(IV) support effect in three different UiO-66-based MOFs was prepared for catalysing cyclohexene oxidation, that is, supported as part of the node (UiO-66-Ti$_{ex}$), attached to the node (Ti-UiO-66) and on a catecholate organic linker (UiO-66-Cat-Ti).[38] The results suggested that Ti-UiO-66 exhibited greater catalytic turnover numbers than UiO-66-Cat-Ti and UiO-66-Ti$_{ex}$.

Gas-phase atomic layer deposition (ALD)[39] was adopted by Hupp *et al.* in a Zr-MOF, NU-1000, to introduce Zn(II) and Al(III) to the Zr_6 clusters.[40, 41] With this method, the nodes of NU-1000 were then selectively functionalized with cobalt sulfide *via* ALD in MOFs (AIM) to obtain CoS-AIM, which is catalytically active for selective hydrogenation of *m*-nitrophenol to *m*-aminophenol.[42] The uniform and precise installation of Ni ions on the node of NU-1000 leads to the formation of Ni-AIM, which exhibits an efficient catalytic activity toward gas-phase hydrogenation upon activation.[43] Besides the AIM method,[43, 44] solvothermal deposition in MOFs (SIM) process was also studied to deposit other transition metals on the Zr-node of NU-1000.[45-47] For example, Mo(VI) oxide was deposited on the Zr_6 node of NU-1000 *via* condensed-phase deposition, namely SIM.[45] The as-synthesized porous heterogeneous catalyst, MoSIM, shows the catalytic activity toward the epoxidation of cyclohexene. They also deposited Co(II) ions at aqua and hydroxo sites in thin film NU-1000 grown on conducting glass substrates by ALD that showed promising electrocatalytic activity for water oxidation.[48] An electrophilic single-site d^0 Zr–benzyl catalytic moiety was embedded in a mesoporous Hf-MOF (Hf-NU-1000), leading to the formation of Hf-NU-1000-ZrBn that worked as a promising single-component catalyst for ethylene and stereoregular 1-hexene polymerization.[49] However, it is critical to understand how the newly deposited species and the MOF couple to govern the active material properties. By the combination of local and long-range structure probes, such as X-ray absorption spectroscopy, pair distribution function analysis and difference envelope density analysis, with electron microscopy imaging and computational modelling, some groups resolved the precise atomic structure

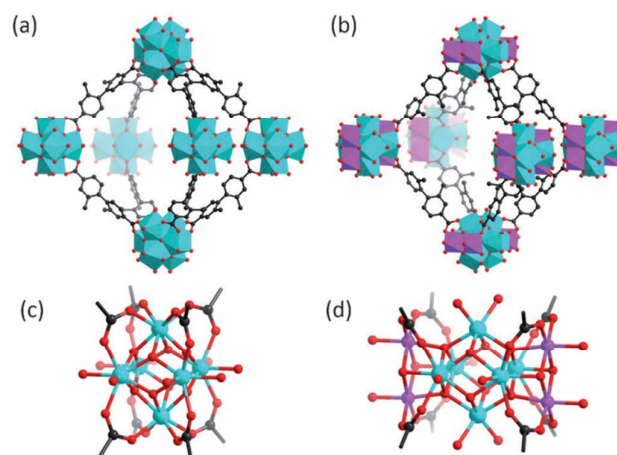of newly deposited metal-oxo species deposited in NU-1000 through ALD.[50, 51]

Fig. 1 a) The structure of PCN-700; b) the structure of PCN-800-(Ni); c) the Zr_6 cluster in PCN-700; d) the Zr_6Ni_4 cluster in PCN-800(Ni) showing the incorporated Ni and migrated carboxylate ligands. Pink Ni; blue Zr; red O; black C; H atoms are omitted for clarity. Reproduced with permission from ref. 55.

Besides, a heterobimetallic Co–Al complex was immobilized onto NU-1000 using a simple solution-based deposition procedure.[52] After heating treatment, the organic ligand of the complex were completely removed without affecting the structural integrity of NU-1000, leading to the formation of a Co–Al oxide cluster. The CoAl-functionalized NU-1000 samples catalyse the oxidation of benzyl alcohol to benzaldehyde with *tert*-butyl hydroperoxide as a stoichiometric oxidant. Density functional theory calculations were performed to elucidate the detailed structures of the Co–Al active sites on the Zr_6-nodes, and a Co-mediated catalytic mechanism is proposed.

Hupp and coworkers demonstrated that the –OH groups on the Zr_6 clusters of UiO-66 can be metalated with redox-active V(V) ions to generate V-UiO-66.[53] The metalated V-UiO-66 displays high selectivity in the vapour-phase oxidative dehydrogenation of cyclohexene for benzene under low-conversion conditions. By increasing the number of ALD cycles, three UiO-66 derivatives with Ni(II) deposited on the Zr_6 nodes of UiO-66 were synthesized *via* an ALD-like process.[54] Upon activation, all three materials exhibit enhanced catalytic activities for ethylene hydrogenation.

In 2015, Zhou *et al.* reported the preparation of bimetallic MOFs, PCN-800(M), based on decanuclear Zr_6M_4 (M = Co or Ni) clusters through cooperative cluster metalation and ligand migration.[55] The 8-connected $[Zr_6O_4(OH)_8(H_2O)_4]$ cluster in PCN-700 was converted to a bimetallic $[Zr_6M_4O_8(OH)_8(H_2O)_8]$ cluster by the reaction of M(II) with the μ_3-OH and H_2O groups (Fig. 1). On the other hand, ligand migration occurred in which a Zr–carboxylate bond dissociates to form a M–carboxylate bond. This single-crystal to single-crystal transformation was recorded by successive single-crystal X-ray diffraction analyses. This work not only offers a powerful tool to functionalize Zr-MOFs with other metals, but structurally elucidates the

formation mechanism of the resulting heterometallic MOFs. Furthermore, In(III) was metalated into PCN-700 to produce PCN-800(In), which exhibits excellent catalytic activity in the cyclotrimerization of acetaldehyde at room temperature under solvent-free condition.

In 2016, Lin *et al.* reported the Co- or Fe-functionalized UiO materials and Zr-MTBC (MTBC = methane-tetrakis(p-biphenylcarboxylate)) through the deprotonation of μ_3-OH or μ_2-OH sites in Zr-clusters with *n*-BuLi followed by reactions with cobalt(II) and iron(II) salts in THF.[56, 57] As single-site solid catalysts, the as-synthesized UiO-CoCl and UiO-FeBr show high activity and reusability for a series of organic reactions,[56] for instance, chemoselective borylation, silylation and amination of sp^3 C–H bonds. The unique coordination environments of Co/Fe centres of the Zr$_6$ clusters as well as the pore structures of UiO-MOF play important roles in controlling the rate and chemoselectivity of these organic transformations. Furthermore, a Ce$_6$-based MOF (Ce-btc, btc = 1,3,5-benzenetricarboxylate) that was modelled using the structure of MOF-808, and activated by sequential deprotonation with LiCH$_2$SiMe$_3$ and reduction with pinacolborane to result in a MOF-supported Ce-hydride catalyst for several important organic transformations.[58] Additionally, the Zr$_6$(μ_3-O)$_4$(μ_3-OH)$_4$(HCOO)$_6$ nodes in MOF-808 can be converted to the [Zr$_6$(μ_3-O)$_4$(μ_3-OH)$_4$Cl$_{12}$]$^{6-}$ nodes and then to the organometallic [Zr$_6$(μ_3-O)$_4$(μ_3-OLi)$_4$(Me)$_n$]$^{6-}$ (n = 6 or 12) nodes, which provides an efficient catalyst for ethylene polymerization.[59]

Owing to the high stability of Zr-MOFs and the ease of functionalizing Zr-clusters with other transition metal ions, we anticipate that Zr-MOFs may offer a versatile platform for the synthesis of highly active MOFs for catalytic transformations. As earth-abundant metal catalysts are critically desired for sustainable chemical synthesis, it is a promising approach to construct bimetallic clusters into a MOF by means of zirconium cluster as structural support and other transition metals as active sites.

2.3. The modification of metal clusters with inorganic acidic sites

Another alternative method to obtain MOF catalysts is to modify the metal nodes with typical inorganic acidic sites, such as sulfonic and phosphate groups.[60-62] Yaghi *et al.* reported the superacidity in a sulfated MOF, MOF-808-2.5SO$_4$ (Zr$_6$O$_5$(OH)$_3$(btc)$_2$(SO$_4$)$_{2.5}$(H$_2$O)$_{2.5}$) (Fig. 2),[60] which was produced by treating the microcrystalline form of MOF-808 (MOF-808-P, Zr$_6$O$_5$(OH)$_3$(btc)$_2$(HCOO)$_5$(H$_2$O)$_2$)[63] with aqueous sulfuric acid. MOF-808-2.5SO$_4$ represents the first superacid in MOFs with a Hammett acidity function $H_0 \leq -14.5$, which can be assigned to the presence of zirconium-bound sulfate structurally characterized using single-crystal X-ray diffraction analysis. MOF-808-2.5SO$_4$ was found to be catalytically active in various acid-catalysed reactions including Friedel–Crafts acylation, esterification and isomerization, as well as in the transformation from methyl cyclopentane to various hydrocarbons.
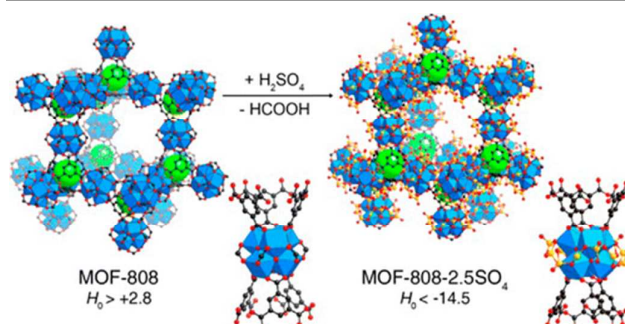

Fig. 2 The structural transformation from MOF-808 to MOF-808-2.5SO$_4$. Reproduced with permission from ref. 60.

Furthermore, Ma *et al.* combined a Brønsted acid MOF with Lewis acid centres to afford MIL-101-Cr-SO$_3$H·Al(III).[64] It demonstrates excellent catalytic behaviour in a series of fixed-bed reactions owing to the synergy between the Brønsted acid framework and the Al(III) Lewis acid sites.

2.4. The modification of metal clusters with molecular catalysts

The fourth method is to functionalize the metal nodes with molecular catalysts. In 2009, Fischer *et al.* reported the postsynthetic functionalization of 1,1'-ferrocenediyl-dimethylsilane to the exposed OH-groups that bridge the metal centres of MIL-53(Al). The as-synthesized (1,1'-ferrocenediyl-dimethylsilane)$_{0.25}$@MIL-53(Al) was tested as a redox catalyst for liquid-phase benzene oxidation with aqueous hydrogen peroxide (30%).[65] Although the conversion was low, the proof of concept for turning MIL-53(Al) into a redox-active functional material was demonstrated. Farha *et al.* immobilised (bpy)Ni^{II} fragments and iridium pincer complex in NU-1000 by solvent assisted ligand-incorporation (SALI), respectively.[66, 67] The resultant framework proved to be stable under the conditions required to activate the Ir-pincer, and further spectroscopic measurements suggested the formation of the catalytically active iridium dihydride.[67] The Ir-pincer modified NU-1000 shows catalytic activity toward the condensed phase hydrogenation of a liquid alkene and possesses enhanced activity compared to a homogeneous counterpart. Additionally, the Ir-pincer immobilised inside NU-1000 operated as an efficient heterogeneous catalyst under flow conditions. In 2017, Zhang *et al.* immobilized a labile dicobalt cluster into a Fe-MOF as coordinative guests, leading to the formation of a thermal-, water-, and alkaline-stable MOF [Fe$_3$(μ_3-O)(bdc)$_3$]$_4$[Co$_2$(na)$_4$(L^T)$_2$]$_3$ (MCF-49, Hna = nicotinic acid, L^T = terminal ligand, Fig. 3).[68] It exhibits extraordinarily high electrocatalytic oxygen evolution activity in water (pH = 13). This result would be insightful for future design and synthesis of new MOF catalysts.

Besides, a halogenated BODIPY (boron-dipyrromethene) ligand was postsynthetically appended to the Zr$_6$ nodes of NU-1000 as a powerful photosensitizer.[69] The BODIPY/MOF material was used as a heterogeneous photocatalyst to produce singlet oxygen under green LED irradiation. The singlet oxygen selectively detoxifies the sulfur mustard

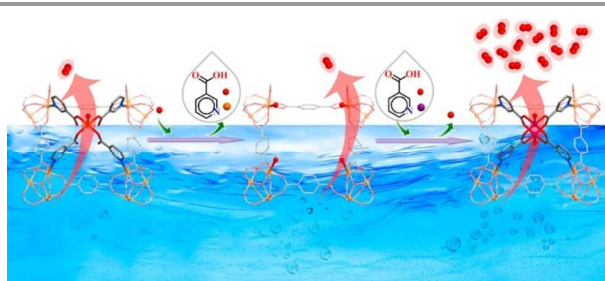simulant, 2-chloroethyl ethyl sulfide, to the less toxic sulfoxide product (2-chloroethyl ethyl sulfoxide).

Fig. 3 The immobilization of a labile dicobalt cluster into a Fe-MOF used as a electrocatalyst toward oxygen evolution. Reproduced with permission from ref. 68.

However, the metal nodes often locate in the corners of a pore, which are difficultly accessible to substrate molecules. In this sense, the substrate conversion may be low because the Lewis acid catalytic sites are not easily reached to the included molecules. Furthermore, the coordination sites of metal nodes are not always available for bonding with reactant molecules, leading to a low catalytic efficiency. As a result, it is full of opportunism to employ MOFs as catalysts with catalytic sites on metal nodes.

3. MOF catalysts with catalytic sites immobilized in organic moieties

The availability of various organic linkers also makes it possible to construct MOFs with ones that containing catalytic sites as the struts, for example, metalloporphyrins,[70-72] metallosalens,[73, 74] and urea.[75, 76] This is an easy and effective method to construct MOF catalysts, in which the assembly of organic fragments bearing high-density active sites into 3D frameworks may provide an ideal system to possess the catalytic activity. In this section, the synthetic strategies and progress of stable MOF catalysts possessing catalytic sites within organic linkers are discussed (Table 2): i) organic linkers with catalytic sites as struts; ii) the organic functional groups appended to the organic linkers; and iii) the rational design of organic linkers with molecular catalysts.

3.1. Organic linkers with catalytic sites as struts

Since the discovery of the heme-containing enzymes, cytochrome P450, the catalytic activities of metalloporphyrin complexes has been extensively investigated.[77] In fact, metalloporphyrins are the active sites in monooxygenases that efficiently oxidize various substrates under mild conditions, which are ideal catalytic struts to construct MOFs owing to their rigidity and well-studied catalytic behaviours.[78-80] Furthermore, the catalytic behaviours of porphyrinic MOFs can be tuned by modulating the metal sites of porphyrin moieties and tailoring the environments of pores, which were comprehensively reviewed for biomimetic catalysis.[81-83]

In 2012, Zhou *et al.* employed Fe-TCPP (TCPP = tetrakis(4-carboxyphenyl)porphyrin) as a heme-like ligand and Zr_6 clusters as nodes for the assembly of stable Zr-MOFs. A 3D

Table 2 The summary of MOF catalysts with catalytic sites immobilized in organic moieties

MOF	Active site	Reaction	Ref.
PCN-222(Fe) (or MMPF-6)	Fe-TCPP	oxidation of THB and ABTS[a]	84,85
PCN-222	TCPP	CO_2 reduction	87
PCN-224(Co)	Co-TCPP	CO_2 cycloaddition	88
Ir-PMOF-1(Zr)	Ir-TCPP	O–H insertion	90
Ir-PMOF-1(Hf)	Ir-TCPP	Si–H insertion	91
PCN-223(Fe)	Fe-TCPP	hetero-Diels–Alder reaction	92
MOF-525	TCPP	oxidative hydroxylation of arylboronic acids	94
MOF-525-Mn	Mn-TCPP	epoxidation of alkenes	95
FJI-H6(Cu), FJI-H7(Cu)	Cu-TBPP[b]	CO_2 cycloaddition	96
PCN-222-Pd(II)	Pd-TCPP	Heck reaction	97
1-TFA	Pd pincer	hydrogenation of benzaldehydes	98
Al-PMOF	TCPP	H_2 generation	99
Al-ATA-Ni MOF	ATA-Ni, TCPP	O_2 evolution	100
PCN-602(Mn)	Mn-TCPP	halogenation of hydrocarbons	102
CMIL-1, CMIL-2	L-proline	asymmetric aldol reactions	108
UiO-67-NHPro, UiO-68-NHPro	L-proline	diastereoselective aldol addition	109
S-MIL-101(Cr)	L-phenylalanine-derived diamine	asymmetric aldol reactions	112
MIL-101-Cr–NH–RSO₃H	alkylsulfonate	condensation of 1,2-diamines	113
Al-MIL-101-NH-peptide, In-MIL-68-NH-peptide, Zr-UiO-66-NH-peptide	peptide	asymmetric aldol reaction	114
UiO-67-Squar/bpdc	squaramide	Friedel–Crafts reactions	115
UiO-67(dcppy)-COOH	–COOH	methanolysis of epoxides	116
Ir/Re/ Ru doped UiO-67	Ir, Re, and Ru complexes	water oxidation, CO_2 reduction, and organic transformations	117
bpy-UiO-Ir or bpy-UiO-Pd	Ir or Pd complexes	C–H borylation of arenes or dehydrogenation of substituted cyclohexenones	118
Pd(II) doped UiO-67	Pd complex	Heck and Suzuki–Miyaura coupling reactions	120,121
Ru–Pt@UIO-67	Ru and Pt complexes	hydrogen generation	122
UiO-67-Ru(bpy)₃	Ru complex	aerobic oxidation of arylboronic acids	123
Cp*Rh@UiO-67	Cp*Rh-based complex	CO_2 reduction	124
Zr-MOF-bpy-CuBr₂	Cu complex	oxidation of cyclooctene	125
Pt@1, Pt@1	Ir complex and Pt NPs	hydrogen generation	126

ARTICLE

Cp*Ir-modified Zr-MOFs	Cp*Ir complexes	water oxidation	127
BPV-MOF-Ir, mBPV-MOF-Ir, and mPT-MOF-Ir	Ir complex	tandem organic transformations via directed C–H activation	128
MOF-Co	Co complex	alkene hydrogenation and hydroboration, aldehyde/ketone hydroboration, and arene C–H borylation	129
BINAP-MOF·Rh, BINAP-dMOF·Rh	Rh complexes	asymmetric organic transformations	130,131
UiO-66-[FeFe](dcbdt)(CO)$_6$, [FeFe]@ZrPF	Fe complex	hydrogen generation	133,134
UiO-66-CrCAT	Cr complex	alcohol oxidation	135
UiO-66-PdTCAT	Pd complex	Regioselective C–H oxidation	136
ZrBDSO$_3$-Hg	Hg^{2+} and –SO$_3$H	acetylene hydration	137
UiO-66-M(CO)$_3$, UiO-67-M(CO)$_3$ (M = Mo, Cr)	Mo or Cr complexes	epoxidation of cyclooctene	138
Mo@UiOs	Mo complex	epoxidation of olefin	139
UiO-66-sal-MoD, UiO-66-PI-MoD, UiO-66-PC-MoD	Mo complexes	epoxidation of olefins	140
NUPF–1–RuCO	RuCO	intermolecular C(sp^3)–H amination	141
(NNN)-M-Zr-MOF (M = Rh, Ir)	Rh or Ir pincer complexes	cascade condensation–hydrogenation	142
Ir-Zr-MOF	Ir complex	N-alkylation of amines with alcohols	143
Zr-NDC-NH$_2$-[LRh]BF$_4$^{c}	Rh complex	cascade olefination/hydrogenation reactions of aldehydes	144
UiO66–NH$_2$–[IrL]^d	Ir pincer complex	hydrogenation of aromatic compounds	145
sal-M-MOF (M = Fe, Co)	Fe or Co complexes	alkene hydrogenation	146
UiO-68–2CH$_3$-L^e	Ir–NHC	isomerisation of 1-octen-3-ol	147
Rh-metalated E$_2$-MOF	Rh(I) complexes	additions of arylboronic acids	148
Ni@(Fe)MIL-101	nickel complex	ethylene dimerization	149
NacNac-M-MOF (M = Fe, Cu, Co)	Fe, Cu, Co complexes	C–H amination and hydrogenation	150
PCN-700-BPYDC(Cu)-TPDC-R$_2$	Cu complex	aerobic alcohol oxidation	152
Cyt C@CYCU-3D	Cyt C	oxidation of ABTS and o-phenylenediamine	154

^{a} THB = 1,2,3-trihydroxybenzene, ^{b} H$_6$TBPP = 4',4''',4''''',4'''''''-(porphyrin-5,10,15,20-tetrayl)tetrakis([1,10-biphenyl]-4-carboxylic acid), ^{c} LRh = Rh complex, ^{d} IrL = iridium pincer complex, ^{e} L = Ir–NHC functionalized terphenyl-4,4''-dicarboxylate.

highly stable mesoporous MOF, PCN-222(Fe), was successfully synthesized, which contains a 1D open channels with a

diameter of up to 3.7 nm (Fig. 4).[84] Kinetic studies demonstrated that an activated sample of PCN-222(Fe) exhibited peroxidase-like biomimetic catalytic activity. PCN-222(Fe) can catalyse the oxidation of a family of substrates with both excellent substrate binding affinity and catalytic activity, which are superior to hemin in aqueous media. In the same year, Ma and coworkers also reported a porous metal–metalloporphyrin framework, MMPF-6,[85] which has the same structure with PCN-222(Fe) and MOF-545-Fe[86] construct by an Fe(III)-metalated porphyrin linker and a secondary binding unit of a zirconium oxide cluster. MMPF-6 demonstrated an interesting peroxidase activity comparable to that of the heme protein myoglobin and exhibited solvent adaptability of retaining the peroxidase activity in an organic solvent. In addition, PCN-222 can effectively capture and further reduce CO_2 with high efficiency under visible-light irradiation in the presence of TEOA as a sacrificial agent.[87]
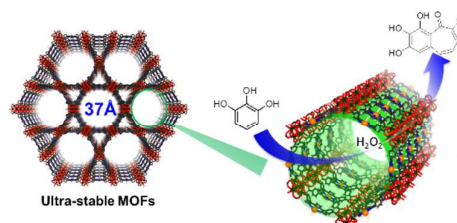

Fig. 4 Peroxidase-like oxidation reaction of pyrogallol catalysed by PCN-222(Fe), in which pyrogallol is oxidized to purpurogallin by hydrogen peroxide. Reproduced with permission from ref. 84.

As a continuation, Zhou *et al.* obtained another family of highly stable porous porphyrin-based Zr-MOFs, namely PCN-224 (no metal, Ni, Co, Fe), by adopting a linker eliminations approach.[88] The Zr$_6$ cluster in PCN-224 series is 6-connected node with D_{3d} symmetry, which is different from 12-connected Zr$_6$ cluster with O_h symmetry in UiO-66 and 8-connected Zr$_6$ cluster with D_{4h} symmetry in PCN-222. Remarkably, PCN-224(Co) shows high catalytic activity toward the CO_2/epoxide coupling reaction and can be used as a recoverable heterogeneous catalyst. Furthermore, size-dependent cellular uptake of PCN-224 for photodynamic therapy (PDT) was observed owing to the photosensitizer of porphyrinic fragments.[89] The catalytic behaviour of stable Ir-PMOF-1(Zr), an isostructure of PCN-224, was evaluated by the O–H insertion reaction of alcohols and phenols.[90] In addition, Ir-PMOF-1(Zr) can be easily recycled and reused without significant loss of catalytic activity. Ir-PMOF-1(Hf), as an isostructure of Ir-PMOF-1(Zr), features high chemoselectivity towards primary silanes among primary, secondary and tertiary silanes in the carbenoid insertion reaction into Si–H bonds.[91]

In 2014, Zhou *et al.* reported another porphyrinic Zr-MOF with shp-a topology, PCN-223,[92] through a kinetically controlled synthetic process, which constructed from the hexagonal prismatic 12-connected Zr$_6$ cluster via an unusual disordered arrangement. After postsynthetic treatment, cationic PCN-223(Fe) was afforded, which can be used as an

excellent recyclable heterogeneous catalyst for the hetero-Diels–Alder reaction. In addition, Zhou *et al.* demonstrated a facile one-pot synthetic method to construct highly stable porous PPN-24(Fe) containing metalloporphyrin fragment, which also exhibits great catalytic activity for the oxidation of ABTS (2,2'-azino-bis-(3-ethylbenzthiazoline-6-sulfonic acid)) in the presence of H_2O_2.[93]

MOF-525 was utilized as a photoredox catalyst toward the oxidative hydroxylation of arylboronic acids in the presence of air and triethylamine under green LED light irradiation,[94] and MOF-525-Mn was used as catalyst for the alkene epoxidation under mild conditions using molecular oxygen.[95] Moreover, MOF-525 series displays a superior catalytic activity for these reactions over the corresponding homogeneous counterpart. Two isostructural porphyrin Zr and Hf MOFs (FJI-H6 and FJI-H7) with 2.5 nm cubic cages were synthesized.[96] Cu(II) can be embed into the open porphyrin rings by a single-crystal to single-crystal transformation. Additionally, FJI-H6(Cu) and FJI-H7(Cu) exhibit promising catalytic activities to convert CO_2 and epoxides into cyclic carbonates under low temperature and pressure.

In 2016, Jiang and coworkers reported a catalytic Heck reaction system based on Pd(II)-porphyrinic MOF, PCN-222-Pd(II), to generate highly fluorescent product in the presence of Cu(II).[97] In the system, the achieved signal enlargement toward Cu(II) with high sensitivity not only takes advantage of a stronger binding affinity of Cu(II) over Pd(II) to the N atoms from the porphyrin fragment, but also a rapid Pd(0)-catalysed Heck-reaction triggered by the addition of Cu(II) ion. PCN-222-Pd(II) sensor possesses much higher selectivity toward Cu(II) than Co(II), Ni(II), and Cd(II) due to the significantly higher affinity of Cu(II) to porphyrin. In addition, it is facile to separate the sensor from the system and free up Cu(II) ion by simple HCl treatment. This work may open up a new opportunity for MOF applications in the detection of metal ions in complex environments.

Besides, diphosphine pincer ligands were widely used in homogeneous catalysis owing to their rigid coordination and tunability. Wade *et al.* reported a porous MOF $Zr_6O_4(OH)_4(L-PdX)_3$, named as 1-X,[98] which was constructed from Pd diphosphinite pincer complexes ($[L-PdX]^{4-} = [(2,6-(OPAr_2)_2C_6H_3)PdX]^{4-}$, Ar = p-$C_6H_4CO_2^-$, X = Cl, I). Furthermore, the reaction of 1-X with $PhI(O_2CCF_3)_2$ facilitates $I^-/CF_3CO_2^-$ ligand exchange to generate 1-TFA. The as-synthesized 1-TFA is an active and recyclable heterogeneous catalyst for transfer hydrogenation of benzaldehydes with formic acid as a hydrogen source.

MOFs based on Al-carboxylate coordination chemistry also exhibit thermally and chemically stable and catch increasing attention as promising heterogeneous catalysts. Rosseinsky *et al.* reported a water-stable porous porphyrin Al-MOF, namely Al-PMOF, which is a photocatalyst for hydrogen generation from water under visible light.[99] The aluminium-based MOF, Al-ATA MOF, made from 2-aminoterephthalate (ATA) is a photocatalyst for oxygen evolution. This MOF can be modified by incorporating Ni(II) ions into the pores by means of coordination to the amino sites, and the resulting MOF, Al-

ATA-Ni MOF, is an efficient photocatalyst for overall water splitting.[100] In Al-ATA-Ni MOF, the Ni(II) cation coordinated to the amino group of ATA serves as the hydrogen evolution site and enhances the oxygen evolution at the benzene ring bearing the amino group.

A base-resistant MOF, namely PCN-602, was constructed with 12-connected $[Ni_8(OH)_4(H_2O)_2Pz_{12}]$ (Pz = pyrazolate) cluster[101] and a pyrazolate-based porphyrin ligand under the guidance of the reticular synthesis strategy.[102] As a heterogeneous MOF catalyst, the Mn(III)-porphyrinic PCN-602 presents high catalytic activity for the C–H bond halogenation reaction of inert hydrocarbons in a basic system, significantly outperforming its homogeneous counterpart. More importantly, the base resistance of PCN-602 series greatly broadens the application scope of MOFs as catalysts.

3.2. The organic functional groups appended to the organic linkers

From a synthetic viewpoint, another mode to provide specific organic moieties for catalysis is to append organic functional groups to the framework of MOFs,[103] which is motivated by the observation that the catalytic activity of several organocatalysts arises from small discrete units such as pyrrolidine,[104] urea,[105] and so on.[106, 107] Some of these organic functional groups-functionalized MOFs further reduce the gap with enzymes by the incorporation of peptide moieties inside the MOF cavities, thereby providing a typical apoenzyme environment.

Kim and coworkers reported an efficient method to prepare chiral porous MOFs by postsynthetic modification of a preassembled achiral MOF. In their work, L-proline (Pro)-based chiral ligands were attached to the open metal coordination sites of MIL-101(Cr) to form CMIL-1 and CMIL-2.[108] The resulting chiral CMIL-1 and CMIL-2 exhibited remarkable catalytic activities in asymmetric aldol reactions, including much higher enantioselectivity than the chiral L-proline-based ligands themselves. The *N*-tert-butyloxycarbonyl protected proline functionalized dicarboxylate linkers were employed by Kaskel *et al.* to produce catalytically active MOFs, UiO-67-NHPro and UiO-68-NHPro, for diastereoselective aldol addition.[109]

The direct synthesis of free sulfonic acid functionalized MIL-101(Cr) was studied by Kitagawa group[110] and Gascon group.[111] The as-synthesized HSO_3-MIL-101(Cr) can be further post-modified with chiral amino acid derived diamine organocatalysts through an acid–base interaction.[112] The diamine immobilized on HSO_3-MIL-101(Cr) material exhibits high *ee* values for the asymmetric aldol condensation of various linear ketones and aromatic aldehydes. An alkylsulfonate functionalized MOF, MIL-101-Cr–NH–RSO$_3$H, was synthesized which exhibits a high catalytic activity and recycling performance for the condensation of 1,2-diamines with benzyl.[113]

Canivet *et al.* explored the modification of bioderived chiral moieties inside MOF cavities by microwave-assisted post-synthetic modification method.[114] In their work, enantiopure peptides were anchored inside the dcavities of Al-MIL-101-

NH$_2$, In-MIL-68-NH$_2$ and Zr-UiO-66-NH$_2$. A single amino acid and various oligopeptides can be grafted with yields up to 60% after the microwave-assisted coupling-deprotection sequence. Furthermore, no racemization of the peptide occurs during the grafting-deprotection process inside MOF cavities by this methodology. This allows the design of a library of functional hybrid solids with confined asymmetric active groups combining high chiral graft density and diversity. Enantiopure peptide-functionalized MOFs were used as catalysts in the asymmetric aldol reaction between acetone and 4-nitrobenzaldehyde. In addition, a leaching test suggests that no active units were released in the solution during the catalytic reaction.

McGuirk and co-workers demonstrated the incorporation of an acidic hydrogen-bond-donating squaramide moiety into a mixed-strut UiO-67 derivative (UiO-67-Squar/bpdc),[115] which can be used as a heterogeneous catalyst for Friedel–Crafts reactions between unsubstituted indole and β-nitroalkenes. By preventing detrimental self-association, the active state of the organocatalyst can be maintained, leading to enhanced activity. Ma *et al.* described the successful insertion of gaseous carbon dioxide into the aryl C–H bonds of the backbone of UiO-67(dcppy) to generate –COOH groups by methylrhodium(I) in DMA (dcppy = 2-phenylpyridine-5,4'-dicarboxylic acid).[116] The resultant UiO-67(dcppy)-COOH serves as a solid state Brønsted acid catalyst for efficiently catalysing the methanolysis of epoxides.

3.3. The rational design of organic linkers with molecular catalysts

Sunlight is the most attractive and abundant renewable energy source to satisfy mankind's future energy needs. More and more artificial photosynthetic systems were built to harvest solar energy and to enable visible-light-driven organic synthesis. In recent years, continuous effort has been devoted to exploring molecular systems (such as, [Ru(bpy)$_3$]$^{2+}$ and [Ir(ppy)$_2$(bpy)]$^+$ derivatives (bpy = 2,2'-bipyridine and ppy = 2-phenylpyridine)) for energy harvesting and visible-light-driven organic transformations due to the easy adjustment of their structure/property. In this section, the encapsulation of molecular catalysts into MOFs through ligand design will be introduced.

In 2011, Lin *et al.* incorporated Ir, Re, and Ru complexes into the UiO framework by a mix-and-match strategy (Fig. 5).[117] The obtained Ir/Re/Ru doped UiO-67 are highly effective catalysts for a range of reactions related to solar energy utilization, including water oxidation, photocatalytic CO$_2$ reduction and visible light-driven organic transformations. As heterogeneous catalysts, they can not only facilitate catalyst recycling and reuse but provide mechanistic insights into the reactions. Furthermore, the modular nature of bipyridyl chelating sites combined with different molecular catalysts allows further fine tuning and optimization to produce highly active heterogeneous catalysts.[118-125] Moreover, Pt nanoparticles were loaded into [Ir(ppy)$_2$(bpy)]$^+$-derived UiO species,[126] which serve as effective photocatalysts for H$_2$ evolution by synergistic photoexcitation of MOF frameworks

and electron injection into Pt nanoparticles. Stable UiO series, possessing carboxylic-acid-functionalized bipyridyl-type linkers with open chelating groups, are versatile platforms for the preparation of heterogeneous catalysts.[127-129] Additionally, Lin and coworkers synthesized a chiral Zr-MOF, BINAP-MOF, based on a BINAP-derived dicarboxylate linker (BINAP = 2,2'-bis(diphenylphosphino)-1,1'-binaphthyl). After post-synthetic metalation of Ru and Rh complexes, a family of single-site solid catalysts for a broad scope of asymmetric organic transformations was afforded.[130, 131]
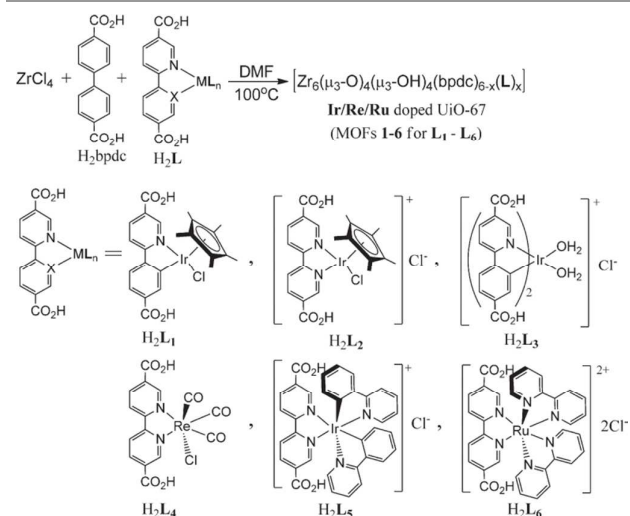

Fig. 5 Synthesis of Doped UiO-67. Reproduced with permission from ref. 117.

A molecular proton reduction catalyst [FeFe](dcbdt)(CO)$_6$ (dcbdt = 1,4-dicarboxylbenzene-2,3-dithiolate) with structural similarities to [FeFe]-hydrogenase active sites[132] was incorporated into a highly robust Zr-MOF, UiO-66, by Cohen and Ott *et al.* with a postsynthetic exchange (PSE) method.[133] Notably, the PSE method is crucial as direct solvothermal synthesis fails to give the functionalized MOF. Furthermore, MOF-[FeFe](dcbdt)(CO)$_6$ was used as a catalyst for photochemical hydrogen evolution in water at pH 5, in conjunction with [Ru(bpy)$_3$]$^{2+}$ as a photosensitizer and ascorbate as an electron donor. By coordinating biomimetic [Fe$_2$S$_2$] active sites ([(í-SCH$_2$)$_2$NC(O)C$_5$H$_4$N]–[Fe$_2$(CO)$_6$]) with porphyrin fragments in a robust Zr-MOF, a new material, [FeFe]@ZrPF, acting both as a photosensitizer and a hydrogen-evolution catalyst was isolated.[134]

Later, Cohen *et al.* prepared a highly robust UiO-66 bearing isolated monocatecholato metal sites on the strut of organic linkers with PSE route. Furthermore, metalation of the catechol functionality residing in the MOFs led to the formation of Fe- and Cr-monocatecholato species.[135] The Cr-metalated UiO-66 was tested as catalyst for the oxidation of alcohols to ketones using a wide range of substrates, which exhibits high activity and is completely recyclable and reusable.

In 2015, the incorporation of 2,3-dimercaptoterephthalate (thiocatecholate, TCAT) into UiO-66 was achieved by PSE method.[136] The anionic, electron-donating thiocatecholato

motif offers a good platform to obtain site-isolated and coordinatively unsaturated soft metal sites in a robust MOF architecture. Metalation of the thiocatechol group with palladium yields Pd-mono(thiocatecholato) fragments within these MOFs, which was used as heterogeneous catalysts for regioselective functionalization of sp^2 C–H bond and can be efficiently recycled. Similarly, Hg(II) was anchored to thiol (–SH) groups within a Zr-MOF, which was further oxidized to acidic sulfonate functions by H_2O_2 for catalysing acetylene hydration at room temperature.[137]

The organic linkers in UiO-66 and UiO-67 also can be modified to arenetricarbonyl metal complexes, [–phM(CO)$_3$–] and [–biphM(CO)$_3$–] (ph = phenylene, biph = biphenylene, M = Mo, Cr) by a chemical vapour deposition treatment of M(CO)$_6$. The resulting UiO-66-M(CO)$_3$ and UiO-67-M(CO)$_3$ are highly active and selective catalysts for cyclooctene epoxidation with *tert*-butyl hydroperoxide (TBHP) as an oxidant.[138] Catalytic activities of these complexes are enhanced with increasing the pore sizes of Zr-based MOFs. After the post-synthetic modification of amino-functionalised UiO series with salicylaldehyde, a molybdenum complex was immobilised, which is active and reusable catalysts for epoxidation of olefins with TBHP or H_2O_2 as an oxidant.[139, 140] Du *et al.* reported a flexible mesoporous amido-based metal–porphyrinic Zr-MOF, NUPF-1, which could be easily post-metallized with [Ru$_3$(CO)$_{12}$] and thus be used as a heterogeneous catalyst for intermolecular C(sp^3)–H amination with good size-selectivity and recyclability.[141]

Rasero-Almansa and coworkers described the postsynthetic modification of Zr-MOFs possessing UiO structure with chiral NNN-pincer ligands on the basis of aminopyridineimines, and the subsequent formation of (NNN)-M-Zr-MOF complexes (M = Rh or Ir).[142-144] The Zr sites (Lewis) and amine and amide groups located in the linkers made (NNN)-M-Zr-MOF act as a bifunctional acid and base catalyst for condensation reactions. Further combination with the Rh/Ir NNN-pincer fragments resulted in a multifunctional Zr–base–transition metal catalyst for one-pot cascade condensation–hydrogenation reactions, and direct N-alkylation of amines with alcohols. In addition, the multifunctional catalysts retain their crystallinity even after the reaction, and they can be separated easily from the reaction mixture by filtration and reused several times without a significant loss in activity. To modify UiO-66 with an iridium pincer complex active phase, a heterogeneous catalyst was obtained and used for the direct hydrogenation of aromatic compounds under mild conditions.[145] The catalyst was found to be highly active and reusable, giving similar reactivity and selectivity for at least five cycles.

A robust and porous Zr-MOF with UiO topology, namely sal-MOF, was obtained using a salicylaldimine (sal)-derived dicarboxylate bridging linker.[146] Postsynthetic metalation of this sal-MOF with FeCl$_2$ or CoCl$_2$ followed by treatment with NaBEt$_3$H in THF resulted in the formation of Fe- and Co-functionalized MOFs (sal-M-MOF, M = Fe or Co). The resulting sal-M-MOF bearing the Fe/Co-sal fragments are highly active single-site solid catalysts for alkene hydrogenation and can be readily recycled and reused. A iridium N-heterocyclic carbene (NHC) metallolinker was introduced into a UiO-68 analogue by direct synthesis and postsynthetic exchange.[147] The two materials exhibited good catalytic activity and recyclability for the isomerisation of an allylic alcohol. These results demonstrate that UiO-68 is an ideal MOF for creating advanced catalytic materials.

Lin *et al.* designed a chiral diene-based Zr-MOF of the UiO structure, E$_2$-MOF, and performed the postsynthetic metalation of E$_2$-MOF with Rh(I) complexes to produce highly active and enantioselective single-site solid catalysts.[148] Treatment of E$_2$-MOF with [RhCl(C$_2$H$_4$)$_2$]$_2$ afforded a highly enantioselective catalyst for 1,4-additions of arylboronic acids to α,β-unsaturated ketones. Moreover, a highly efficient catalyst for the asymmetric 1,2-additions of arylboronic acids to aldimines would be isolated when E$_2$-MOF was treated with Rh(acac)(C$_2$H$_4$)$_2$. In addition, E$_2$-MOF·Rh(acac) can be recycled and reused without loss of yield and enantioselectivity.

Amino group on the walls of stable MOFs can serve as an ideal starting platform for postsynthetic functionalization.[149, 150] Lin *et al.* installed the β-diketiminate (NacNac) fragment into a Zr-MOF of UiO-topology.[150] Further metalation of the NacNac-MOF with earth-abundant metal salts generated the desired MOF-supported NacNac-M complexes (M = Fe, Cu, and Co). The obtained NacNac-M-MOF catalysts exhibit enhanced catalytic activities for the intramolecular sp^3 C–H amination and alkene hydrogenation compared to their analogous homogeneous catalysts. In addition, all of the NacNac-M-MOF catalysts could be recycled and reused without a noticeable decrease in yield.

Zhou *et al.* employed a stable Zr-MOF with coordinatively unsaturated Zr$_6$ clusters, PCN-700,[151] to perform a comprehensive study on the linker installation method. Guided by the geometrical analysis, twelve linkers with different lengths and substituents were tried to install into a parent PCN-700, leading to 11 new MOFs and each bearing up to three different functional groups in predefined positions.[152] The result suggests that PCN-700 is an ideal platform for systematic variation of pore volume and pore environment by judicious selection of linkers.[152, 153] As a result, a catalytic system for the oxidation of aerobic alcohol was built in PCN-700 through the sequential installation of BPYDC(Cu) and TPDC-R$_2$ (BPYDC = 2,2'-bipyridne-5,5'-dicarboxylate, TPDC = terphenyl-4,4''-dicarboxylate, R = Me, Ph, or Hex, Fig. 6). The as-synthesized PCN-700-BPYDC(Cu)-TPDC-R$_2$ shows high catalytic activity and tunable size selectivity. Overall, these results exemplify the advantage of the linker installation strategy in the pore environment engineering of stable MOFs with multiple functional groups, giving an unparalleled level of control. Precise placement of multiple functional groups into a highly ordered MOF platform allows tailoring the pore environment, which is highly required for practical applications. Furthermore, they employed a new method, i.e., linker labilization, to increase the MOF porosity and pore size through the splitting of a pro-labile-linker and the removal of the linker fragments by acid treatment.[154] The linker labilization approach can create controllable hierarchical-pore

architectures in stable MOFs, which facilitates the diffusion and adsorption process of guest molecules to improve the performances of MOFs in catalysis.
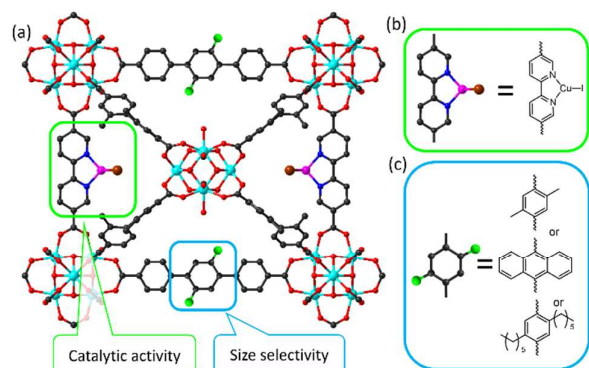

Fig. 6 (a) Size-selective catalytic system for aerobic alcohol oxidation reaction built in PCN-700 through linker installation. (b,c) Structure of catalytic centre and size-selective moiety. Coordinated CH$_3$CN on the Cu is removed for clarity. Reproduced with permission from ref. 152.

Until now, a number of catalytic sites have been successfully immobilized onto organic fragments to modify the pore surfaces of MOFs, leading to remarkable catalytic efficiency with interesting size and shape-selective properties. On the one hand, it is rational and straightforward method to implant the catalytic centres to organic fragments by means of various organic transformations. On the other hand, the catalytic sites are easily accessed to reactant molecules by immobilizing on the pore surfaces of MOFs.

4. MOF catalysts with catalytic centres encapsulated in the pores

The tunability of pore features (including size, shape, environment and charge type) allows MOFs to be a suitable host matrix for the encapsulation of diverse catalytic centres into the pores (Table 3). To an extent, different window sizes of cavity offers possibility for the encapsulation of catalytic centres that prevent catalytic sites leaching while allowing diffusion of reactants and products. In addition, the environments and charge types of cavity in MOFs also have influences on the interactions between host framework and guests. In this context, it is highly desired to produce stable MOFs for encapsulation of active centres that can maintain framework integrity upon the encapsulation and under the investigated catalytic conditions.

4.1. Stable MOFs with trapped enzyme active centres in pores

Chemists are often inspired by nature in the pursuit of efficient structures when designing new catalysts for chemical transformations. In the previous sections, we have introduced the construction of MOF catalysts by incorporating active sites into the struts of a MOF. The tunable cavity spaces and the functional pore walls of MOFs also provide a promising

opportunity for biomimetic catalysis. Furthermore, the incorporation of the enzyme centres into a suitable MOF

Table 3 The summary of MOF catalysts with catalytic centres encapsulated in the pores

MOF	Active site	Reaction	Ref.
Mn-RTMPyP-encapsulated in *rho*-ZMOF	Mn-RTMPyP	hydrocarbon oxidation	156
hemin@MIL-101(Al)–NH$_2$	hemin	oxidation of TMB^a	157
Mn-TAPP@ZIF-8	Mn-TAPP	epoxidation of olefins	158
MP-11@Tb-mesoMOF	MP-11	oxidation of DTBC^b	159
Mb@Tb-mesoMOF	Mb	oxidation of ABTS and THB	161
HRP@PCN-333(Al), Cyt c@PCN-333(Al), MP-11@PCN-333(Al)	HRP, Cyt c, MP-11	oxidation of ABTS	163
GOx@PCN-888, HRP@PCN-888	GOx, HRP	oxidation of ABTS	164
OPAA@PCN-128y, OPAA@NU-1003	OPAA	hydrolysis of nerve agents	165,166
Mn-salen@MIL-101(Al)	Mn(III)salen complex	epoxidation of dihydronaphthalene	167
MnTD@MIL-101(Cr)	MnTD	water oxidation	168,171
CuPhen/MIL	Cu complexes	oxidation of cycloalkane	169
Ru-alkylidene complexes@(Al)MIL-101-NH$_2$·HCl	Ru-alkylidene complexes	olefin metathesis	170
POM@MOF^c	POM, [Ru(bpy)$_3$]$^{2+}$	H$_2$ generation	172
PW$_{11}$Zn@NH$_2$-MIL-101(Al)	PW$_{11}$Zn	sulfoxidation	173
Co(CO)$_4$⊂Cr-MIL-101	Co(CO)$_4$, Cr(III)	epoxide carbonylation	174
Ru(bpy)$_3$@PCN-99	[Ru(bpy)$_3$]$^{2+}$	aerobic hydroxylation of arylboronic acid	175
Au@ZIF-8	Au NPs	CO oxidation	177
Pt@MIL-101	Pt NPs	ammonia borane hydrolysis, ammonia borane thermal dehydrogenation, CO oxidation	178
Pd/MIL-101	Pd NPs	Suzuki–Miyaura and Ullmann coupling reactions of aryl chlorides	179
Pd/MIL-101(Al)-NH$_2$	Pd NPs	hydrogenation of 5-hydroxymethylfurfural	180
Pd@MIL-88B-NH$_2$(Fe)	Pd NPs	C–H activation/halogenation reaction	181
Pt@UiO-66-NH$_2$	Pt NPs	Hydrogen generation	182
Pd-in-UiO-67, Pd^0/UiO-67	Pd NPs	olefin hydrogenation, aerobic oxidation of alcohols and reduction of nitrobenzene	183
Pd@Ag-in-UiO-67	Pd@Ag NPs	partial-hydrogenation of phenylacetylene	184
Ag@MIL-101	Ag NPs	C–H bond activation of terminal alkynes	185
Co@MIL-53(Al)	Co NPs	Fischer–Tropsch synthesis	186
Pt/MIL-100(Fe)	Pt NPs	Hydrogen generation	187
GOx–MIL-100(Fe)–PtNP	Pt NPs	glucose detection	188
Pt@ZIF-8, Pt@SALEM-2	Pt NPs	hydrogenation of 1-octene and *cis*-cyclohexene	189
CuZn@UiO-bpy	Cu/ZnO$_x$ NPs	hydrogenation of CO$_2$	190
Pt@ZIF-8	Pt NPs	hydrogenation of n-hexene	191,192

^{a} TMB = 3,3,5,5-tetramethylbenzidine, ^{b} DTBC = 3,5-Di-*t*-butylcatechol, ^{c} POM = [P$_2$W$_{18}$O$_{62}$]$^{6-}$, MOF represents [Ru(bpy)$_3$]$^{2+}$-derived UiO series.

cavities not only prevents aggregation, but also renders catalytic centres more accessible to substrates as well as allows a broad range of solution conditions.[155]

As a class of metal complexes used ubiquitously in biological systems, metalloporphyrins were shown to be essential in many enzymatic processes and were encapsulated in the pores of MOFs. Eddaoudi *et al.* reported the utilization of (In-HImDC)-based *rho*-ZMOF as a host for large catalytically active molecules, specifically porphyrins.[156] Furthermore, the porphyrin fragment was metalated, postsynthesis, by various transition metal ions to produce a wide range of metalloporphyrins, which was used as hydrocarbon oxidation catalysts. The amino-containing MOF, MIL-101(Al)–NH$_2$, was used as a host matrix material to anchor hemin and simulate the peptidic microenvironment in the native peroxidase.[157] The as-prepared mimetic peroxidase exhibits catalytic activity toward the oxidation of 3,3,5,5-tetramethylbenzidine (TMB) in the presence of H$_2$O$_2$. ZIF-8 (Zn(MeIM)$_2$, MeIM = 2-methylimidazole) was employed as a host matrix for the accommodation of custom-designed porphyrin molecules *via* hydrogen bonding,[158] in which there is a suitable micro-environment similar to the protein skeleton around the active sites in haemoglobin. The obtained Mn-TAPP@ZIF-8 exhibits an enhanced catalytic efficiency and selectivity compared to the homogeneous complexes, strongly supporting the synergistic effect raised from the H-bond interaction.

Ma and coworkers immobilized microperoxidase-11 (MP-11),[159] cytochrome c (Cyt c)[160] and myoglobin (Mb)[161] into a mesoporous MOF with MTN topology, Tb-mesoMOF,[162] which is composed of Tb$_4$ cluster and triazine-1,3,5-tribenzoate (TATB). The resulting MP-11@Tb-mesoMOF demonstrates superior enzymatic catalysis performances compared to its mesoporous silica counterpart. In 2015, Zhou *et al.* reported a series of water-stable MOFs, namely PCN-332(M) (M = Al(III), Fe(III), Sc(III), V(III), In(III)) and PCN-333(M) (M = Al(III), Fe(III), Sc(III)), with rationally designed ultra-large mesoporous cages that can serve as single-molecule traps (SMTs).[163] Among them, PCN-333(Al) encapsulates three enzymes with different sizes, horseradish peroxidase (HRP), Cyt c and MP-11. After the encapsulation of enzymes in PCN-333(Al), immobilized enzymes show higher catalytic efficiency than free enzymes and recyclability under the same condition, essentially

eliminating enzyme aggregation and leaching. With extraordinarily large pore size and excellent chemical stability, PCN-333 may be promising not only for enzyme encapsulation, but also for entrapment of other nanoscaled functional moieties.

Later, Zhou and co-workers obtained an isoreticular analogue of PCN-333, PCN-888,[164] which was utilized to couple two enzymes into a tandem nanoreactor. PCN-888 contains three types of mesoporous cages: a largest cavity (6.2 nm) can only accommodate one molecule of glucose oxidase (GOx), an intermediate cavity (5.0 nm) can accommodate only one molecule of HRP and a small cavity (2.0 nm) without sufficient size for GOx and HRP remains open as a substrate diffusion pathway. By means of a unique stepwise encapsulation with a specific order (GOx first, followed by HRP, Fig. 7), the coupling of the two enzymes can be realized. The tandem nanoreactor not only exhibits excellent catalytic performances and negligible enzyme leaching, but the catalytic activity can be well-maintained within several catalytic cycles. In addition, the protective effect of PCN-888 on the encapsulated enzymes against trypsin digestion suggests that cage-MOF tandem nanoreactors have great potential to be applied in more complex systems. In addition, a nerve agent detoxifying enzyme, organophosphorus acid anhydrolase (OPAA), were encapsulated into the water-stable Zr-MOF.[165, 166] The work highlights a method for rapid and highly efficient hydrolysis of nerve agents using nanosized enzyme carriers.
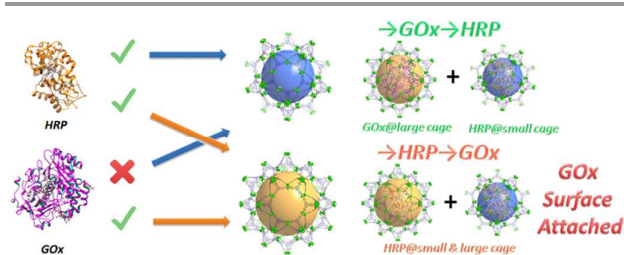

Fig. 7 Graphic representation of the results of the stepwise encapsulation of GOx and HRP with different orders. Reproduced with permission from ref. 164.

4.2. Encapsulation of molecular catalysts into the pores

The presence of mesopores in MIL-101 and its superior stability makes it an ideal platform for the encapsulation of molecular catalysts.[167-170] In 2013, a chiral Mn(III)salen complex was entrapped in MIL-101 to obtain an enantioselective catalyst, Mn-salen@MIL-101(Al).[167] The resulting heterogeneous catalyst shows the same selectivity as the homogeneous complex and is fully recyclable. Das reported the assembly of a highly reactive molecular catalyst into MOF pores, MnTD@MIL-101(Cr) (MnTD = [(terpy)Mn(µ-O)$_2$Mn](terpy)]$^{3+}$, terpy = 2,2':6',2''-terpyridine). The obtained MnTD@MIL-101(Cr) not only exhibited promising water oxidation rates, but maintained the same rate for hours in the presence of KHSO$_5$ as the sacrificial oxidant.[168] In addition, with cerium(IV) ammonium nitrate as an external oxidant, MnTD@MIL-101(Cr) maintains its water oxidation activity for hours and even after a week, under the harsh conditions required for water oxidation (pH = 1).[171] In 2016, Ru-alkylidene

complexes bearing ammonium-tagged NHC ligands were supported inside MIL-101(Al)-NH$_2$·HCl by Chmielewski and coworkers.[170] The resulting materials were used as heterogeneous catalysts in olefin metathesis reactions. Although the catalysts were held inside the MOF cavity by noncovalent forces only, no leaching was observed and heavy metal contamination of the products was found to be below the detection limit of ICP MS (0.02 ppm).

Besides the encapsulation of molecular catalyst in MOFs through ligand design and *in situ* entrapment, the encapsulation of molecular catalysts into the pores by ion interactions were also explored.[172-174] Lin *et al.* developed a charge-assisted self-assembly process for the encapsulation of a polyoxometalate (POM) inside a porous and phosphorescent UiO MOF built from [Ru(bpy)$_3$]$^{2+}$-derived dicarboxylate linkers and Zr$_6$ clusters.[172] The authors hypothesized that the large cavities in the [Ru(bpy)$_3$]$^{2+}$-derived cationic MOF should provide an ideal environment for the encapsulation of functional anionic entities to result in multifunctional materials. As a result, the Wells–Dawson [P$_2$W$_{18}$O$_{62}$]$^{6-}$ ions were loaded into the cavities of this UiO MOF by simply heating a mixture of ZrCl$_4$ and [Ru(bpy)$_3$]$^{2+}$-derived ligand in the presence of POM. The integration of photosensitizing and catalytic proton reduction components in such a POM@MOF assembly enables fast multielectron injection from the photoactive MOF to the encapsulated redox-active POM upon photoexcitation, resulting in efficient visible-light-driven hydrogen production.

In 2016, Zhou and co-workers designed a strictly trigonal-planar linker to produce an anionic bor-MOF, PCN-99, using topology guidance.[175] As a result, the encapsulation of [Ru(bpy)$_3$]$^{2+}$ into PCN-99 through cation exchange was realized due to its anionic nature of framework. Furthermore, Ru(bpy)$_3$@PCN-99 shows photocatalytic activity toward the aerobic hydroxylation of arylboronic acid.

4.3. Encapsulation of metal nanoparticles (NPs) into the pores

In the past decades, noble metal NPs supported on metal oxides, zeolites, mesoporous materials, and activated carbons were widely studied as catalysts. As a new kind of highly-ordered porous materials with tunable size, shape and microenvironment of the pores, MOFs are promising platform for solid heterogeneous catalysts by embedding noble metal NPs into the pores of MOFs which would limit the migration and aggregation of metal clusters/NPs.[176] Here some representative examples with stable MOFs as supports are introduced.

Xu *et al.* reported Au NPs deposited to a zeolite-type MOF, ZIF-8, with high thermal stability (over 500 °C) and large pore size (diameter of 11.6 Å).[177] The pretreated ZIF-8 and desired quantitative volatile organogold complex, (CH$_3$)$_2$Au(acac) (acac = acetylacetonate), were ground uniformly for ~35 min in an agate mortar in air at room temperature. The as-synthesized Au@ZIF-8 was employed as an active catalyst in the gas phase CO oxidation and exhibited considerable activity. Furthermore, they immobilized ultrafine Pt NPs inside the pores of another classical zeolite-type MOF, MIL-101(Cr), without aggregation of

Pt NPs on the external surfaces of framework by using a 'double solvents' method.[178] The resulting Pt@MIL-101(Cr) composite was used for catalytic reactions in all three phases: liquid-phase ammonia borane hydrolysis, solid-phase ammonia borane thermal dehydrogenation, and gas-phase CO oxidation.

Jiang and co-workers used MIL-101(Cr) as the support for palladium NPs to catalyse a water-mediated coupling system.[179] The as-synthesized Pd/MIL-101(Cr) was utilized as heterogeneous catalyst system for the water-mediated Suzuki–Miyaura and Ullmann coupling reactions of aryl chlorides. In addition, Pd/MIL-101(Cr) is stable, not only exhibiting negligible metal leaching, but maintaining high catalytic activities over a number of cycles. Another catalyst of palladium supported amine-functionalized MIL-101, Pd/MIL-101(Al)-NH_2,[180] shows selective hydrogenation of biomass-based 5-hydroxymethylfurfural (HMF) to 2,5-dihydroxymethyl-tetrahydrofuran. Pd@MIL-88B-NH_2(Fe) exhibits highly selective heterogeneous procedures for C–H activation/halogenation reactions.[181]

UiO-66-NH_2 with high stability and visible-light responsive is another ideal matrix for supporting metal NPs to get enhanced photocatalysis. The pre-synthesis of Pt NPs of *ca.* 3 nm were incorporated inside or supported on UiO-66-NH_2, denoted as Pt@UiO-66-NH_2 and Pt/UiO-66-NH_2, respectively.[182] They were used as photocatalysts for production of hydrogen *via* water splitting. Relatively, Pt@UiO-66-NH_2 greatly shortens the electron-transport distance, which is favourable for the electron–hole separation and thereby yields much higher efficiency than that of Pt/UiO-66-NH_2. The involved mechanism was further unveiled by ultrafast transient absorption and photoluminescence technique.

UiO-67 was chosen as the host matrix for the encapsulation of metal NPs because of its high physicochemical stability and tunable functionalities of ligands with 2,2-bipyride moieties to serve as anchor sites for metal atom. Li *et al.* developed to encapsulate palladium precursors through ligand design prior to UiO-67 assembly, achieving uniformly distributed Pd(II) inside the pores of MOFs. The as-prepared Pd(II)-in-UiO-67 was treated under H_2 at 250 °C for 4 h to afford Pd^0-in-UiO-67, which showed excellent shape-selectivity in hydrogenation of olefin and high catalytic efficiencies in aerobic oxidation of alcohols and nitrobenzene reduction.[183] The DMF solution of Pd^0-in-UiO-67 was bubbled with H_2 for 1 h at room temperature, a $AgNO_3$ solution was added under stirring, leading to the growth of Ag on the surface of the embedded Pd NPs. The Pd@Ag core–shell NPs on MOFs was formed by a seed mediated growth strategy (Fig. 8), which can be assigned to the presence of activated physisorbed H atoms on embedded Pd NPs as reducing agents to selectively direct the deposition of Ag onto Pd while minimizing Ag self-nucleation.[184] The as-synthesized Pd@Ag core–shell NPs showed a higher selectivity in the partial hydrogenation of phenylacetylene than their monometallic counterparts, resulting from the surface dilution and electron modification of the surface Pd sites by Ag deposition. In addition, Pd@Ag NPs exhibited an unparalleled high stability and recyclability in the catalytic reactions, which can be

attributed to the nano-confinement effect and the strong metal–support interaction provided by the MOF framework.
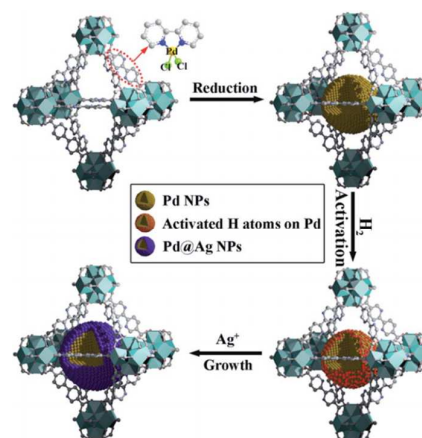

Fig. 8 Schematic illustration of the fabrication of Pd@Ag core–shell NPs encapsulated in the MOF pore. Reproduced with permission from ref. 183.

Besides, other metal NPs immobilized into stable MOFs were also studied.[185-190] For example, UiO-bpy series were used to anchor ultrasmall Cu/ZnO_x NPs in order to prevent the agglomeration of Cu NPs and phase separation between Cu and ZnO_x in MOF-cavity-confined Cu/ZnO_x NPs.[190] The resultant Cu/ZnO_x@MOF catalysts exhibit high activity and 100% selectivity for CO_2 hydrogenation to methanol. Very recently, metal NPs-encapsulated MOFs with controllable spatial localization were realized through employing metal oxide as both the support to load metal NPs and the sacrificial template to grow MOFs.[191, 192] The resultant metal NPs@MOF composites exhibit not only effective selectivity derived from MOF cavities, but also enhanced activity resulting from the spatial regulation of metal NPs as close as possible to the MOF surface.

5. MOFs for biomimetics

In this section, stable MOFs used for biomimetics will be introduced. The structural flexibility of MOFs makes them possible response to various stimuli. For instance, a Cu-MOF reported by Morris *et al.* shows low-pressure selectivity towards nitric oxide through a coordination-driven gating mechanism.[193] Nitric oxide is a crucial signalling molecule with site-specific and concentration-dependent activities. Furukawa and co-workers developed spatiotemporally controllable nitric oxide-releasing platforms based on photoactive porous ZIFs, NOF-1 and NOF-2 (Fig. 9).[194] Increased photoreactivity and adjustable NO release were observed using light irradiation by organizing molecules with poor reactivity into ZIF structures. With this method, the biological relevance of the exogenous NO is evidenced by an intracellular change in calcium concentration, mediated by NO-responsive plasma membrane channel proteins.
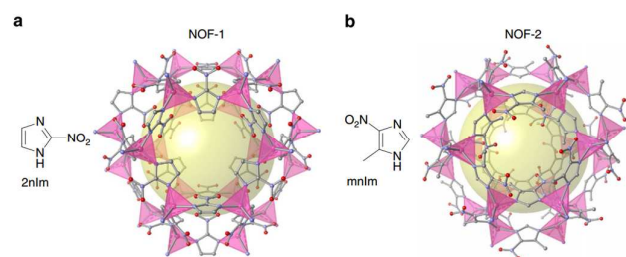
Fig. 9 The nitro-containing imidazole ligands were independently reacted in the presence of zinc ions to form the porous sodalite ZIFs, (a) NOF-1 and (b) NOF-2. Reproduced with permission from ref. 193.

The stereochemical sensing capability of porous $[In(OH)(bdc)]_n$ microcrystals and oriented films toward a series of chemicals was successfully transduced to the photoluminescence emission responses. The biomimetic ''nose'' could distinguish the odors of the analytes based on a pattern recognition method (i.e., principal component analysis).[195] In addition, the tastant interacts stereochemically with poly(acrylic acid) and alters the conformations of $[In(OH)(bdc)]_n$, making it as a biomimetic ''tongue''.[196]

In addition, Mao *et al.* utilized ZIFs as a matrix for coimmobilizing electrocatalysts and dehydrogenases onto the electrode surface, and an integrated electrochemical biosensor is readily formed.[197] Moreover, the biosensor is capable of monitoring dialysate glucose collected from the brain of guinea pigs selectively and in a near real-time pattern. Jiang *et al.* used two iron(III)-based MOFs as efficient peroxidase mimics, which can catalyse the oxidation of different peroxidase substrates by H_2O_2 accompanied with significant colour change in the solution.[198] As a result, a simple and sensitive colorimetric assay was established to detect H_2O_2 and ascorbic acid.

It is a critical challenge in biotechnology to improve the robustness of functional biomacromolecules, which plays an important role in pharmaceuticals, chemical processing and biostorage. Liang and co-workers demonstrated that a series of biomacromolecules including proteins, enzymes and DNA can efficiently induce MOF formation and control the morphology of the resultant porous crystal *via* a biomimetic mineralization process under physiological conditions (Fig. 10).[199] They used two methods (biomimetic mineralisation and controlled co-precipitation) for the preparation of such composite materials.[200] In addition, they investigated natural amino acids[201] and carbohydrates (polysaccharides)[202] as biomimetic crystallization agents for the synthesis of ZIF-8 particles in aqueous solution. The resulting biocomposite can be stable under conditions that would normally decompose many biological macromolecules. Zhu *et al.* reported a facile biomimetic mineralization to entrap thermophilic lipase QLM in the cages of ZIF-8 to generate lipase@ZIF-8.[203] Furthermore, the composite lipase@ZIF-8 was used as catalyst for the hydrolysis of *p*-nitrophenyl caprylate, exhibiting favourable catalytic activity and stability.

Besides, MOFs provide possibility to be used in other biomimetic fields. For instance, Falcaro *et al.* reported that ZIF-

8 and $Ln_2(bdc)_3$ crystalline thin films and patterns can be generated as a result of biomimetic replication directly from protein patterns on various surfaces in aqueous conditions at room temperature.[204] Gassensmith *et al.* used a robust protein template, tobacco mosaic virus (TMV), to regulate the size and shape of as-fabricated ZIF-8 materials.[205] More interestingly, the virus particle underneath ZIF-8 shell can be chemically modified using a standard bioconjugation reaction, exhibiting mass transportation within the MOF shell.
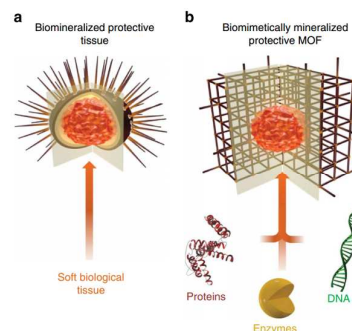

Fig. 10 Schematic illustration of biomimetically mineralized MOF: (a) a sea urchin; a hard porous protective shell that is biomineralized by soft biological tissue and (b) a MOF biocomposite showing a biomacromolecule encapsulated within the porous crystalline shell. Reproduced with permission from ref. 198.

6. Conclusions

MOFs are an emerging class of heterogeneous catalysts with structural tunability and synergistic effects resulting from the coexistence of different types of catalytic centres. However, the chemical stability of MOFs would limit their practical applications because the intactness of their frameworks is guaranteed to allow their catalytic performance to be fully exerted and their reuse. In this review, three types of stable MOF catalysts were discussed in details according to the structural characteristics of MOF materials (metal nodes, organic linkers, and pores). Compared with other traditional systems, stable MOFs possessing a series of advantages, namely, i) highly ordered crystalline structures, ii) high loadings, more uniform and accessible catalytic sites, and iii) enhanced catalytic activity in some cases by providing confined spaces for reactants and eliminating multimolecular catalyst deactivation pathways, represent a kind of promising heterogeneous catalysts. Furthermore, the catalytic centres can be placed in a specific location through the judicious selection of building blocks and rational design of topology networks. This makes the preparation of MOFs more purposeful, which is challenging in synthetic chemistry and material science.

However, the study of stable MOFs as heterogeneous catalysts is still in its infancy. So far, the investigation mainly involved in Zr-MOFs and Cr-MOFs. Meanwhile, ZIF materials were the most popularly used among all MOFs as for biomimetic study, especially ZIF-8. As a result, there is still a strong need to develop new types of materials in the ever-

growing domain of stable MOF materials for catalysis and biomimetics.

Acknowledgements

Conflicts of interest

There are no conflicts of interest to declare.

References

1. H. X. Deng, S. Grunder, K. E. Cordova, C. Valente, H. Furukawa, M. Hmadeh, F. Gandara, A. C. Whalley, Z. Liu, S. Asahina, H. Kazumori, M. O'Keeffe, O. Terasaki, J. F. Stoddart and O. M. Yaghi, *Science*, 2012, **336**, 1018-1023.
2. H. Sato, W. Kosaka, R. Matsuda, A. Hori, Y. Hijikata, R. V. Belosludov, S. Sakaki, M. Takata and S. Kitagawa, *Science*, 2014, **343**, 167-170.
3. Z. C. Hu, B. J. Deibert and J. Li, *Chem. Soc. Rev.*, 2014, **43**, 5815-5840.
4. M. Yoon, R. Srirambalaji and K. Kim, *Chem. Rev.*, 2012, **112**, 1196-1231.
5. I. Nath, J. Chakraborty and F. Verpoort, *Chem. Soc. Rev.*, 2016, **45**, 4127-4170.
6. L. E. Kreno, K. Leong, O. K. Farha, M. Allendorf, R. P. Van Duyne and J. T. Hupp, *Chem. Rev.*, 2012, **112**, 1105-1125.
7. P. Horcajada, R. Gref, T. Baati, P. K. Allan, G. Maurin, P. Couvreur, G. Ferey, R. E. Morris and C. Serre, *Chem. Rev.*, 2012, **112**, 1232-1268.
8. P. Ramaswamy, N. E. Wong and G. K. H. Shimizu, *Chem. Soc. Rev.*, 2014, **43**, 5913-5932.
9. H. Deng, C. J. Doonan, H. Furukawa, R. B. Ferreira, J. Towne, C. B. Knobler, B. Wang and O. M. Yaghi, *Science*, 2010, **327**, 846-850.
10. V. Guillerm, D. Kim, J. F. Eubank, R. Luebke, X. Liu, K. Adil, M. S. Lah and M. Eddaoudi, *Chem. Soc. Rev.*, 2014, **43**, 6141-6172.
11. P. Deria, J. E. Mondloch, O. Karagiaridi, W. Bury, J. T. Hupp and O. K. Farha, *Chem. Soc. Rev.*, 2014, **43**, 5896-5912.
12. D. N. Bunck and W. R. Dichtel, *Chem.–Eur. J.*, 2013, **19**, 818-827.
13. J. S. Qin, S. Yuan, Q. Wang, A. Alsalme and H. C. Zhou, *J. Mater. Chem. A*, 2017, **5**, 4280-4291.
14. C. D. Wu and M. Zhao, *Adv. Mater.*, 2017, **29**, 1605446.
15. S. M. J. Rogge, A. Bavykina, J. Hajek, H. Garcia, A. I. Olivos-Suarez, A. Sepulveda-Escribano, A. Vimont, G. Clet, P. Bazin, F. Kapteijn, M. Daturi, E. V. Ramos-Fernandez, I. X. F. X. Llabres, V. Van Speybroeck and J. Gascon, *Chem. Soc. Rev.*, 2017, **46**, 3134-3184.
16. J. A. Greathouse and M. D. Allendorf, *J. Am. Chem. Soc.*, 2006, **128**, 10678-10679.
17. M. Rimoldi, A. J. Howarth, M. R. DeStefano, L. Lin, S. Goswami, P. Li, J. T. Hupp and O. K. Farha, *ACS Catal.*, 2017, **7**, 997-1014.
18. G. Ferey, *Chem. Soc. Rev.*, 2008, **37**, 191-214.
19. Y. Bai, Y. B. Dou, L. H. Xie, W. Rutledge, J. R. Li and H. C. Zhou, *Chem. Soc. Rev.*, 2016, **45**, 2327-2367.
20. M. Eddaoudi, D. F. Sava, J. F. Eubank, K. Adil and V. Guillerm, *Chem. Soc. Rev.*, 2015, **44**, 228-249.
21. G. Ferey, C. Mellot-Draznieks, C. Serre, F. Millange, J. Dutour, S. Surble and I. Margiolaki, *Science*, 2005, **309**, 2040-2042.
22. A. Henschel, K. Gedrich, R. Kraehnert and S. Kaskel, *Chem. Commun.*, 2008, 4192-4194.
23. Y. K. Hwang, D.-Y. Hong, J.-S. Chang, H. Seo, M. Yoon, J. Kim, S. H. Jhung, C. Serre and G. Férey, *Appl. Catal. A-Gen.*, 2009, **358**, 249-253.
24. J. Kim, S. Bhattacharjee, K. E. Jeong, S. Y. Jeong and W. S. Ahn, *Chem. Commun.*, 2009, 3904-3906.
25. N. V. Maksimchuk, K. A. Kovalenko, V. P. Fedin and O. A. Kholdeeva, *Adv. Synth. Catal.*, 2010, **352**, 2943-2948.
26. W. Liu, J. Huang, Q. Yang, S. Wang, X. Sun, W. Zhang, J. Liu and F. Huo, *Angew. Chem. Int. Ed.*, 2017, **56**, 5512-5516.
27. O. V. Zalomaeva, A. M. Chibiryaev, K. A. Kovalenko, O. A. Kholdeeva, B. S. Balzhinimaev and V. P. Fedin, *J. Catal.*, 2013, **298**, 179-185.
28. M. H. Beyzavi, R. C. Klet, S. Tussupbayev, J. Borycz, N. A. Vermeulen, C. J. Cramer, J. F. Stoddart, J. T. Hupp and O. K. Farha, *J. Am. Chem. Soc.*, 2014, **136**, 15861-15864.
29. M. H. Beyzavi, N. A. Vermeulen, A. J. Howarth, S. Tussupbayev, A. B. League, N. M. Schweitzer, J. R. Gallagher, A. E. Platero-Prats, N. Hafezi, A. A. Sarjeant, J. T. Miller, K. W. Chapman, J. F. Stoddart, C. J. Cramer, J. T. Hupp and O. K. Farha, *J. Am. Chem. Soc.*, 2015, **137**, 13624-13631.
30. P. Li, R. C. Klet, S. Y. Moon, T. C. Wang, P. Deria, A. W. Peters, B. M. Klahr, H. J. Park, S. S. Al-Juaid, J. T. Hupp and O. K. Farha, *Chem. Commun.*, 2015, **51**, 10925-10928.
31. L. T. Hoang, L. H. Ngo, H. L. Nguyen, H. T. Nguyen, C. K. Nguyen, B. T. Nguyen, Q. T. Ton, H. K. Nguyen, K. E. Cordova and T. Truong, *Chem. Commun.*, 2015, **51**, 17132-17135.
32. F. Vermoortele, R. Ameloot, A. Vimont, C. Serre and D. De Vos, *Chem. Commun.*, 2011, **47**, 1521-1523.
33. F. Vermoortele, M. Vandichel, B. Van de Voorde, R. Ameloot, M. Waroquier, V. Van Speybroeck and D. E. De Vos, *Angew. Chem. Int. Ed.*, 2012, **51**, 4887-4890.
34. M. J. Katz, S.-Y. Moon, J. E. Mondloch, M. H. Beyzavi, C. J. Stephenson, J. T. Hupp and O. K. Farha, *Chem. Sci.*, 2015, **6**, 2286-2291.
35. M. J. Katz, J. E. Mondloch, R. K. Totten, J. K. Park, S. T. Nguyen, O. K. Farha and J. T. Hupp, *Angew. Chem. Int. Ed.*, 2014, **53**, 497-501.
36. M. Kim, J. F. Cahill, H. Fei, K. A. Prather and S. M. Cohen, *J. Am. Chem. Soc.*, 2012, **134**, 18082-18088.

37.   Y. Lee, S. Kim, J. K. Kang and S. M. Cohen, *Chem. Commun.*, 2015, **51**, 5735-5738.

38.   H. G. T. Nguyen, L. Mao, A. W. Peters, C. O. Audu, Z. J. Brown, O. K. Farha, J. T. Hupp and S. T. Nguyen, *Catal. Sci. Technol.*, 2015, **5**, 4444-4451.

39.   S. M. George, *Chem. Rev.*, 2010, **110**, 111-131.

40.   J. E. Mondloch, W. Bury, D. Fairen-Jimenez, S. Kwon, E. J. DeMarco, M. H. Weston, A. A. Sarjeant, S. T. Nguyen, P. C. Stair, R. Q. Snurr, O. K. Farha and J. T. Hupp, *J. Am. Chem. Soc.*, 2013, **135**, 10294-10297.

41.   M. Rimoldi, V. Bernales, J. Borycz, A. Vjunov, L. C. Gallington, A. E. Platero-Prats, I. S. Kim, J. L. Fulton, A. B. F. Martinson, J. A. Lercher, K. W. Chapman, C. J. Cramer, L. Gagliardi, J. T. Hupp and O. K. Farha, *Chem. Mater.*, 2017, **29**, 1058-1068.

42.   A. W. Peters, Z. Li, O. K. Farha and J. T. Hupp, *ACS Nano*, 2015, **9**, 8484-8490.

43.   Z. Li, N. M. Schweitzer, A. B. League, V. Bernales, A. W. Peters, A. B. Getsoian, T. C. Wang, J. T. Miller, A. Vjunov, J. L. Fulton, J. A. Lercher, C. J. Cramer, L. Gagliardi, J. T. Hupp and O. K. Farha, *J. Am. Chem. Soc.*, 2016, **138**, 1977-1982.

44.   A. W. Peters, Z. Li, O. K. Farha and J. T. Hupp, *ACS Appl. Mater. Interfaces*, 2016, **8**, 20675-20681.

45.   H. Noh, Y. Cui, A. W. Peters, D. R. Pahls, M. A. Ortuno, N. A. Vermeulen, C. J. Cramer, L. Gagliardi, J. T. Hupp and O. K. Farha, *J. Am. Chem. Soc.*, 2016, **138**, 14720-14726.

46.   S. Ahn, N. E. Thornburg, Z. Li, T. C. Wang, L. C. Gallington, K. W. Chapman, J. M. Notestein, J. T. Hupp and O. K. Farha, *Inorg. Chem.*, 2016, **55**, 11954-11961.

47.   Z. Li, A. W. Peters, V. Bernales, M. A. Ortuno, N. M. Schweitzer, M. R. DeStefano, L. C. Gallington, A. E. Platero-Prats, K. W. Chapman, C. J. Cramer, L. Gagliardi, J. T. Hupp and O. K. Farha, *ACS Cent. Sci.*, 2017, **3**, 31-38.

48.   C. W. Kung, J. E. Mondloch, T. C. Wang, W. Bury, W. Hoffeditz, B. M. Klahr, R. C. Klet, M. J. Pellin, O. K. Farha and J. T. Hupp, *ACS Appl. Mater. Interfaces*, 2015, **7**, 28223-28230.

49.   R. C. Klet, S. Tussupbayev, J. Borycz, J. R. Gallagher, M. M. Stalzer, J. T. Miller, L. Gagliardi, J. T. Hupp, T. J. Marks, C. J. Cramer, M. Delferro and O. K. Farha, *J. Am. Chem. Soc.*, 2015, **137**, 15680-15683.

50.   A. E. Platero-Prats, A. B. League, V. Bernales, J. Ye, L. C. Gallington, A. Vjunov, N. M. Schweitzer, Z. Li, J. Zheng, B. L. Mehdi, A. J. Stevens, A. Dohnalkova, M. Balasubramanian, O. K. Farha, J. T. Hupp, N. D. Browning, J. L. Fulton, D. M. Camaioni, J. A. Lercher, D. G. Truhlar, L. Gagliardi, C. J. Cramer and K. W. Chapman, *J. Am. Chem. Soc.*, 2017, **139**, 10410-10418.

51.   T. Ikuno, J. Zheng, A. Vjunov, M. Sanchez-Sanchez, M. A. Ortuno, D. R. Pahls, J. L. Fulton, D. M. Camaioni, Z. Li, D. Ray, B. L. Mehdi, N. D. Browning, O. K. Farha, J. T. Hupp, C. J. Cramer, L. Gagliardi and J. A. Lercher, *J. Am. Chem. Soc.*, 2017, **139**, 10294-10301.

52.   A. B. Thompson, D. R. Pahls, V. Bernales, L. C. Gallington, C. D. Malonzo, T. Webber, S. J. Tereniak, T. C. Wang, S. P. Desai, Z. Li, I. S. Kim, L. Gagliardi, R. L. Penn, K. W. Chapman, A. Stein, O. K. Farha, J. T. Hupp, A. B. F. Martinson and C. C. Lu, *Chem. Mater.*, 2016, **28**, 6753-6762.

53.   H. G. T. Nguyen, N. M. Schweitzer, C.-Y. Chang, T. L. Drake, M. C. So, P. C. Stair, O. K. Farha, J. T. Hupp and S. T. Nguyen, *ACS Catal.*, 2014, **4**, 2496-2500.

54.   Z. Li, A. W. Peters, J. Liu, X. Zhang, N. M. Schweitzer, J. T. Hupp and O. K. Farha, *Inorg. Chem. Front.*, 2017, **4**, 820-824.

55.   S. Yuan, Y. P. Chen, J. S. Qin, W. G. Lu, X. Wang, Q. Zhang, M. Bosch, T. F. Liu, X. Z. Lian and H. C. Zhou, *Angew. Chem. Int. Ed.*, 2015, **54**, 14696-14700.

56.   K. Manna, P. Ji, Z. Lin, F. X. Greene, A. Urban, N. C. Thacker and W. Lin, *Nat. Commun.*, 2016, **7**, 12610.

57.   P. Ji, K. Manna, Z. Lin, A. Urban, F. X. Greene, G. Lan and W. Lin, *J. Am. Chem. Soc.*, 2016, **138**, 12234-12242.

58.   P. Ji, T. Sawano, Z. Lin, A. Urban, D. Boures and W. Lin, *J. Am. Chem. Soc.*, 2016, **138**, 14860-14863.

59.   P. Ji, J. B. Solomon, Z. Lin, A. Johnson, R. F. Jordan and W. Lin, *J. Am. Chem. Soc.*, 2017, **139**, 11325-11328.

60.   J. Jiang, F. Gandara, Y. B. Zhang, K. Na, O. M. Yaghi and W. G. Klemperer, *J. Am. Chem. Soc.*, 2014, **136**, 12844-12847.

61.   J. W. Chen, Z. G. Zhang, Z. B. Bao, Y. Su, H. B. Xing, Q. W. Yang and Q. L. Ren, *ACS Appl. Mater. Interfaces*, 2017, **9**, 9772-9777.

62.   M. Yabushita, P. Li, T. Islamoglu, H. Kobayashi, A. Fukuoka, O. K. Farha and A. Katz, *Ind. Eng. Chem. Res.*, 2017, **56**, 7141-7148.

63.   H. Furukawa, F. Gandara, Y. B. Zhang, J. Jiang, W. L. Queen, M. R. Hudson and O. M. Yaghi, *J. Am. Chem. Soc.*, 2014, **136**, 4369-4381.

64.   B. Y. Li, K. Y. Leng, Y. M. Zhang, J. J. Dynes, J. Wang, Y. F. Hu, D. X. Ma, Z. Shi, L. K. Zhu, D. L. Zhang, Y. Y. Sun, M. Chrzanowski and S. Q. Ma, *J. Am. Chem. Soc.*, 2015, **137**, 4243-4248.

65.   M. Meilikhov, K. Yusenko and R. A. Fischer, *J. Am. Chem. Soc.*, 2009, **131**, 9644-9645.

66.   S. T. Madrahimov, J. R. Gallagher, G. Zhang, Z. Meinhart, S. J. Garibay, M. Delferro, J. T. Miller, O. K. Farha, J. T. Hupp and S. T. Nguyen, *ACS Catal.*, 2015, **5**, 6713-6718.

67.   M. Rimoldi, A. Nakamura, N. A. Vermeulen, J. J. Henkelis, A. K. Blackburn, J. T. Hupp, J. F. Stoddart and O. K. Farha, *Chem. Sci.*, 2016, **7**, 4980-4984.

68.   J. Q. Shen, P. Q. Liao, D. D. Zhou, C. T. He, J. X. Wu, W. X. Zhang, J. P. Zhang and X. M. Chen, *J. Am. Chem. Soc.*, 2017, **139**, 1778-1781.

69.   A. Atilgan, T. Islamoglu, A. J. Howarth, J. T. Hupp and O. K. Farha, *ACS Appl. Mater. Interfaces*, 2017, **9**, 24555-24560.

70.   P. Deria, D. A. Gomez-Gualdron, I. Hod, R. Q. Snurr, J. T. Hupp and O. K. Farha, *J. Am. Chem. Soc.*, 2016, **138**, 14449-14457.

71.   J. S. Qin, D. Y. Du, M. Li, X. Z. Lian, L. Z. Dong, M. Bosch, Z. M. Su, Q. Zhang, S. L. Li, Y. Q. Lan, S. Yuan and H. C. Zhou, *J. Am. Chem. Soc.*, 2016, **138**, 5299-5307.

72.   S. Yuan, J. S. Qin, L. F. Zou, Y. P. Chen, X. Wang, Q. Zhang and H. C. Zhou, *J. Am. Chem. Soc.*, 2016, **138**, 6636-6642.

73.   F. Song, C. Wang, J. M. Falkowski, L. Ma and W. Lin, *J. Am. Chem. Soc.*, 2010, **132**, 15390-15398.

74.   C. Zhu, G. Yuan, G. Chen, Z. Yang and Y. Cui, *J. Am. Chem. Soc.*, 2012, **134**, 8058-8061.

75.   J. M. Roberts, B. M. Fini, A. A. Sarjeant, O. K. Farha, J. T. Hupp and K. A. Scheidt, *J. Am. Chem. Soc.*, 2012, **134**, 3334-3337.

76.   Z. Ju, S. Yan and D. Yuan, *Chem. Mater.*, 2016, **28**, 2000-2010.

77.   C. M. Che, V. K. Lo, C. Y. Zhou and J. S. Huang, *Chem. Soc. Rev.*, 2011, **40**, 1950-1975.

78. M. Zhao, S. Ou and C. D. Wu, *Acc. Chem. Res.*, 2014, **47**, 1199-1207.

79. W. Y. Gao, M. Chrzanowski and S. Ma, *Chem. Soc. Rev.*, 2014, **43**, 5841-5866.

80. Z. Y. Guo and B. L. Chen, *Dalton Trans.*, 2015, **44**, 14574-14583.

81. Z. Y. Gu, J. Park, A. Raiff, Z. W. Wei and H. C. Zhou, *ChemCatChem*, 2014, **6**, 67-75.

82. M. Zhang, Z.-Y. Gu, M. Bosch, Z. Perry and H.-C. Zhou, *Coord. Chem. Rev.*, 2015, **293-294**, 327-356.

83. Y. Chen and S. Q. Ma, *Dalton Trans.*, 2016, **45**, 9744-9753.

84. D. W. Feng, Z. Y. Gu, J. R. Li, H. L. Jiang, Z. W. Wei and H. C. Zhou, *Angew. Chem. Int. Ed.*, 2012, **51**, 10307-10310.

85. Y. Chen, T. Hoang and S. Q. Ma, *Inorg. Chem.*, 2012, **51**, 12600-12602.

86. W. Morris, B. Volosskiy, S. Demir, F. Gandara, P. L. McGrier, H. Furukawa, D. Cascio, J. F. Stoddart and O. M. Yaghi, *Inorg. Chem.*, 2012, **51**, 6443-6445.

87. H. Q. Xu, J. Hu, D. Wang, Z. Li, Q. Zhang, Y. Luo, S. H. Yu and H. L. Jiang, *J. Am. Chem. Soc.*, 2015, **137**, 13440-13443.

88. D. Feng, W. C. Chung, Z. Wei, Z. Y. Gu, H. L. Jiang, Y. P. Chen, D. J. Darensbourg and H. C. Zhou, *J. Am. Chem. Soc.*, 2013, **135**, 17105-17110.

89. J. Park, Q. Jiang, D. Feng, L. Mao and H. C. Zhou, *J. Am. Chem. Soc.*, 2016, **138**, 3518-3525.

90. H. Cui, Y. Wang, Y. Wang, Y.-Z. Fan, L. Zhang and C.-Y. Su, *CrystEngComm*, 2016, **18**, 2203-2209.

91. Y. Wang, H. Cui, Z. W. Wei, H. P. Wang, L. Zhang and C. Y. Su, *Chem. Sci.*, 2017, **8**, 775-780.

92. D. W. Feng, Z. Y. Gu, Y. P. Chen, J. Park, Z. W. Wei, Y. J. Sun, M. Bosch, S. Yuan and H. C. Zhou, *J. Am. Chem. Soc.*, 2014, **136**, 17714-17717.

93. L. Zou, D. Feng, T. F. Liu, Y. P. Chen, S. Fordham, S. Yuan, J. Tian and H. C. Zhou, *Chem. Commun.*, 2015, **51**, 4005-4008.

94. T. Toyao, N. Ueno, K. Miyahara, Y. Matsui, T. H. Kim, Y. Horiuchi, H. Ikeda and M. Matsuoka, *Chem. Commun.*, 2015, **51**, 16103-16106.

95. J. W. Brown, Q. T. Nguyen, T. Otto, N. N. Jarenwattananon, S. Glöggler and L.-S. Bouchard, *Catal. Commun.*, 2015, **59**, 50-54.

96. J. Zheng, M. Wu, F. Jiang, W. Su and M. Hong, *Chem. Sci.*, 2015, **6**, 3466-3470.

97. Y. Z. Chen and H. L. Jiang, *Chem. Mater.*, 2016, **28**, 6698-6704.

98. S. A. Burgess, A. Kassie, S. A. Baranowski, K. J. Fritzsching, K. Schmidt-Rohr, C. M. Brown and C. R. Wade, *J. Am. Chem. Soc.*, 2016, **138**, 1780-1783.

99. A. Fateeva, P. A. Chater, C. P. Ireland, A. A. Tahir, Y. Z. Khimyak, P. V. Wiper, J. R. Darwent and M. J. Rosseinsky, *Angew. Chem. Int. Ed.*, 2012, **51**, 7440-7444.

100. Y. An, Y. Y. Liu, P. F. An, J. C. Dong, B. Y. Xu, Y. Dai, X. Y. Qin, X. Y. Zhang, M. H. Whangbo and B. B. Huang, *Angew. Chem. Int. Ed.*, 2017, **56**, 3036-3040.

101. K. Wang, X. L. Lv, D. Feng, J. Li, S. Chen, J. Sun, L. Song, Y. Xie, J. R. Li and H. C. Zhou, *J. Am. Chem. Soc.*, 2016, **138**, 914-919.

102. X. L. Lv, K. Wang, B. Wang, J. Su, X. Zou, Y. Xie, J. R. Li and H. C. Zhou, *J. Am. Chem. Soc.*, 2017, **139**, 211-217.

103. J. V. Alegre-Requena, E. Marques-Lopez, R. P. Herrera and D. D. Diaz, *CrystEngComm*, 2016, **18**, 3985-3995.

104. D. J. Lun, G. I. Waterhouse and S. G. Telfer, *J. Am. Chem. Soc.*, 2011, **133**, 5806-5809.

105. P. W. Siu, Z. J. Brown, O. K. Farha, J. T. Hupp and K. A. Scheidt, *Chem. Commun.*, 2013, **49**, 10920-10922.

106. J. Chen, R. Liu, H. Gao, L. Chen and D. Ye, *J. Mater. Chem. A*, 2014, **2**, 7205-7213.

107. Y. Luan, Y. Qi, H. Gao, R. S. Andriamitantsoa, N. Zheng and G. Wang, *J. Mater. Chem. A*, 2015, **3**, 17320-17331.

108. M. Banerjee, S. Das, M. Yoon, H. J. Choi, M. H. Hyun, S. M. Park, G. Seo and K. Kim, *J. Am. Chem. Soc.*, 2009, **131**, 7524-7525.

109. C. Kutzscher, G. Nickerl, I. Senkovska, V. Bon and S. Kaskel, *Chem. Mater.*, 2016, **28**, 2573-2580.

110. G. Akiyama, R. Matsuda, H. Sato, M. Takata and S. Kitagawa, *Adv. Mater.*, 2011, **23**, 3294-3297.

111. J. Juan-Alcañiz, R. Gielisse, A. B. Lago, E. V. Ramos-Fernandez, P. Serra-Crespo, T. Devic, N. Guillou, C. Serre, F. Kapteijn and J. Gascon, *Catal. Sci. Technol.*, 2013, **3**, 2311-2318.

112. A. L. W. Demuynck, M. G. Goesten, E. V. Ramos-Fernandez, M. Dusselier, J. Vanderleyden, F. Kapteijn, J. Gascon and B. F. Sels, *ChemCatChem*, 2014, **6**, 2211-2214.

113. R. S. Andriamitantsoa, J. Wang, W. Dong, H. Gao and G. Wang, *RSC Adv.*, 2016, **6**, 35135-35143.

114. J. Bonnefoy, A. Legrand, E. A. Quadrelli, J. Canivet and D. Farrusseng, *J. Am. Chem. Soc.*, 2015, **137**, 9409-9416.

115. C. M. McGuirk, M. J. Katz, C. L. Stern, A. A. Sarjeant, J. T. Hupp, O. K. Farha and C. A. Mirkin, *J. Am. Chem. Soc.*, 2015, **137**, 919-925.

116. W. Y. Gao, H. Wu, K. Leng, Y. Sun and S. Ma, *Angew. Chem. Int. Ed.*, 2016, **55**, 5472-5476.

117. C. Wang, Z. G. Xie, K. E. deKrafft and W. L. Lin, *J. Am. Chem. Soc.*, 2011, **133**, 13445-13454.

118. K. Manna, T. Zhang and W. Lin, *J. Am. Chem. Soc.*, 2014, **136**, 6566-6569.

119. T. Liu, D. Q. Li, S. Y. Wang, Y. Z. Hu, X. W. Dong, X. Y. Liu and C. M. Che, *Chem. Commun.*, 2014, **50**, 13261-13264.

120. L. Chen, S. Rangan, J. Li, H. Jiang and Y. Li, *Green Chem.*, 2014, **16**, 3978-3985.

121. H. Fei and S. M. Cohen, *Chem. Commun.*, 2014, **50**, 4810-4812.

122. C.-C. Hou, T.-T. Li, S. Cao, Y. Chen and W.-F. Fu, *J. Mater. Chem. A*, 2015, **3**, 10386-10394.

123. X. Yu and S. M. Cohen, *Chem. Commun.*, 2015, **51**, 9880-9883.

124. M. B. Chambers, X. Wang, N. Elgrishi, C. H. Hendon, A. Walsh, J. Bonnefoy, J. Canivet, E. A. Quadrelli, D. Farrusseng, C. Mellot-Draznieks and M. Fontecave, *ChemSusChem*, 2015, **8**, 603-608.

125. T. Toyao, K. Miyahara, M. Fujiwaki, T.-H. Kim, S. Dohshi, Y. Horiuchi and M. Matsuoka, *J. Phys. Chem. C*, 2015, **119**, 8131-8137.

126. C. Wang, K. E. deKrafft and W. Lin, *J. Am. Chem. Soc.*, 2012, **134**, 7211-7214.

127. C. Wang, J. L. Wang and W. Lin, *J. Am. Chem. Soc.*, 2012, **134**, 19895-19908.

128. K. Manna, T. Zhang, F. X. Greene and W. Lin, *J. Am. Chem. Soc.*, 2015, **137**, 2665-2673.

129. T. Zhang, K. Manna and W. Lin, *J. Am. Chem. Soc.*, 2016, **138**, 3241-3249.

130. J. M. Falkowski, T. Sawano, T. Zhang, G. Tsun, Y. Chen, J. V. Lockard and W. Lin, *J. Am. Chem. Soc.*, 2014, **136**, 5213-5216.
131. T. Sawano, N. C. Thacker, Z. Lin, A. R. McIsaac and W. Lin, *J. Am. Chem. Soc.*, 2015, **137**, 12241-12248.
132. G. Caserta, S. Roy, M. Atta, V. Artero and M. Fontecave, *Curr. Opin. Chem. Biol.*, 2015, **25**, 36-47.
133. S. Pullen, H. Fei, A. Orthaber, S. M. Cohen and S. Ott, *J. Am. Chem. Soc.*, 2013, **135**, 16997-17003.
134. K. Sasan, Q. P. Lin, C. Y. Mao and P. Y. Feng, *Chem. Commun.*, 2014, **50**, 10390-10393.
135. H. Fei, J. Shin, Y. S. Meng, M. Adelhardt, J. Sutter, K. Meyer and S. M. Cohen, *J. Am. Chem. Soc.*, 2014, **136**, 4965-4973.
136. H. Fei and S. M. Cohen, *J. Am. Chem. Soc.*, 2015, **137**, 2191-2194.
137. K. K. Yee, Y. L. Wong, M. Zha, R. Y. Adhikari, M. T. Tuominen, J. He and Z. Xu, *Chem. Commun.*, 2015, **51**, 10941-10944.
138. M. Saito, T. Toyao, K. Ueda, T. Kamegawa, Y. Horiuchi and M. Matsuoka, *Dalton Trans.*, 2013, **42**, 9444-9447.
139. M. Kaposi, M. Cokoja, C. H. Hutterer, S. A. Hauser, T. Kaposi, F. Klappenberger, A. Pothig, J. V. Barth, W. A. Herrmann and F. E. Kuhn, *Dalton Trans.*, 2015, **44**, 15976-15983.
140. J. Tang, W. Dong, G. Wang, Y. Yao, L. Cai, Y. Liu, X. Zhao, J. Xu and L. Tan, *RSC Adv.*, 2014, **4**, 42977-42982.
141. L. Xu, Y. P. Luo, L. Sun, Y. Xu, Z. S. Cai, M. Fang, R. X. Yuan and H. B. Du, *Chem. Eur. J.*, 2016, **22**, 6268-6276.
142. A. M. Rasero-Almansa, A. Corma, M. Iglesias and F. Sánchez, *ChemCatChem*, 2013, **5**, 3092-3100.
143. A. M. Rasero-Almansa, A. Corma, M. Iglesias and F. Sánchez, *ChemCatChem*, 2014, **6**, 1794-1800.
144. A. M. Rasero-Almansa, A. Corma, M. Iglesias and F. Sánchez, *ChemCatChem*, 2014, **6**, 3426-3433.
145. A. M. Rasero-Almansa, A. Corma, M. Iglesias and F. Sánchez, *Green Chem.*, 2014, **16**, 3522-3527.
146. K. Manna, T. Zhang, M. Carboni, C. W. Abney and W. Lin, *J. Am. Chem. Soc.*, 2014, **136**, 13182-13185.
147. F. Carson, E. Martinez-Castro, R. Marcos, G. Gonzalez Miera, K. Jansson, X. Zou and B. Martin-Matute, *Chem. Commun.*, 2015, **51**, 10864-10867.
148. T. Sawano, P. Ji, A. R. McIsaac, Z. Lin, C. W. Abney and W. Lin, *Chem. Sci.*, 2015, **6**, 7163-7168.
149. J. Canivet, S. Aguado, Y. Schuurman and D. Farrusseng, *J. Am. Chem. Soc.*, 2013, **135**, 4195-4198.
150. N. C. Thacker, Z. Lin, T. Zhang, J. C. Gilhula, C. W. Abney and W. Lin, *J. Am. Chem. Soc.*, 2016, **138**, 3501-3509.
151. S. Yuan, W. G. Lu, Y. P. Chen, Q. Zhang, T. F. Liu, D. W. Feng, X. Wang, J. S. Qin and H. C. Zhou, *J. Am. Chem. Soc.*, 2015, **137**, 3177-3180.
152. S. Yuan, Y. P. Chen, J. S. Qin, W. G. Lu, L. F. Zou, Q. Zhang, X. Wang, X. Sun and H. C. Zhou, *J. Am. Chem. Soc.*, 2016, **138**, 8912-8919.
153. S. Yuan, L. F. Zou, H. X. Li, Y. P. Chen, J. S. Qin, Q. Zhang, W. G. Lu, M. B. Hall and H. C. Zhou, *Angew. Chem. Int. Ed.*, 2016, **55**, 10776-10780.
154. S. Yuan, L. Zou, J. S. Qin, J. Li, L. Huang, L. Feng, X. Wang, M. Bosch, A. Alsalme, T. Cagin and H. C. Zhou, *Nat. Commun.*, 2017, **8**, 15356.

155. X. Lian, Y. Fang, E. Joseph, Q. Wang, J. Li, S. Banerjee, C. Lollar, X. Wang and H. C. Zhou, *Chem. Soc. Rev.*, 2017, **46**, 3386-3401.
156. M. H. Alkordi, Y. Liu, R. W. Larsen, J. F. Eubank and M. Eddaoudi, *J. Am. Chem. Soc.*, 2008, **130**, 12639-12641.
157. F. X. Qin, S. Y. Jia, F. F. Wang, S. H. Wu, J. Song and Y. Liu, *Catal. Sci. Technol.*, 2013, **3**, 2761-2768.
158. W. J. Zhang, Y. Wang, Y. Leng, P. B. Zhang, J. Zhang and P. P. Jiang, *Catal. Sci. Technol.*, 2016, **6**, 5848-5855.
159. V. Lykourinou, Y. Chen, X. S. Wang, L. Meng, T. Hoang, L. J. Ming, R. L. Musselman and S. Ma, *J. Am. Chem. Soc.*, 2011, **133**, 10382-10385.
160. Y. Chen, V. Lykourinou, C. Vetromile, T. Hoang, L. J. Ming, R. W. Larsen and S. Ma, *J. Am. Chem. Soc.*, 2012, **134**, 13188-13191.
161. Y. Chen, V. Lykourinou, T. Hoang, L. J. Ming and S. Ma, *Inorg. Chem.*, 2012, **51**, 9156-9158.
162. Y. K. Park, S. B. Choi, H. Kim, K. Kim, B. H. Won, K. Choi, J. S. Choi, W. S. Ahn, N. Won, S. Kim, D. H. Jung, S. H. Choi, G. H. Kim, S. S. Cha, Y. H. Jhon, J. K. Yang and J. Kim, *Angew. Chem. Int. Ed.*, 2007, **46**, 8230-8233.
163. D. Feng, T. F. Liu, J. Su, M. Bosch, Z. Wei, W. Wan, D. Yuan, Y. P. Chen, X. Wang, K. Wang, X. Lian, Z. Y. Gu, J. Park, X. Zou and H. C. Zhou, *Nat. Commun.*, 2015, **6**, 5979.
164. X. Z. Lian, Y. P. Chen, T. F. Liu and H. C. Zhou, *Chem. Sci.*, 2016, **7**, 6969-6973.
165. P. Li, S. Y. Moon, M. A. Guelta, S. P. Harvey, J. T. Hupp and O. K. Farha, *J. Am. Chem. Soc.*, 2016, **138**, 8052-8055.
166. P. Li, S. Y. Moon, M. A. Guelta, L. Lin, D. A. Gomez-Gualdron, R. Q. Snurr, S. P. Harvey, J. T. Hupp and O. K. Farha, *ACS Nano*, 2016, **10**, 9197-9182.
167. T. Bogaerts, A. Van Yperen-De Deyne, Y. Y. Liu, F. Lynen, V. Van Speybroeck and P. Van Der Voort, *Chem. Commun.*, 2013, **49**, 8021-8023.
168. B. Nepal and S. Das, *Angew. Chem. Int. Ed.*, 2013, **52**, 7224-7227.
169. Y. Chen, B. Fan, N. Lu and R. Li, *Catal. Commun.*, 2015, **64**, 91-95.
170. A. Chołuj, A. Zieliński, K. Grela and M. J. Chmielewski, *ACS Catal.*, 2016, **6**, 6343-6349.
171. R. E. Hansen and S. Das, *Energy Environ. Sci.*, 2014, **7**, 317-322.
172. Z. M. Zhang, T. Zhang, C. Wang, Z. Lin, L. S. Long and W. Lin, *J. Am. Chem. Soc.*, 2015, **137**, 3197-3200.
173. D. Juliao, A. C. Gomes, M. Pillinger, R. Valenca, J. C. Ribeiro, B. de Castro, I. S. Goncalves, L. Cunha Silva and S. S. Balula, *Eur. J. Inorg. Chem.*, 2016, 5114-5122.
174. H. D. Park, M. Dinca and Y. Roman-Leshkov, *ACS Cent. Sci.*, 2017, **3**, 444-448.
175. X. Wang, W. Lu, Z. Y. Gu, Z. Wei and H. C. Zhou, *Chem. Commun.*, 2016, **52**, 1926-1929.
176. Q. Yang, Q. Xu and H. L. Jiang, *Chem. Soc. Rev.*, 2017, **46**, 4774-4808.
177. H. L. Jiang, B. Liu, T. Akita, M. Haruta, H. Sakurai and Q. Xu, *J. Am. Chem. Soc.*, 2009, **131**, 11302-11303.
178. A. Aijaz, A. Karkamkar, Y. J. Choi, N. Tsumori, E. Ronnebro, T. Autrey, H. Shioyama and Q. Xu, *J. Am. Chem. Soc.*, 2012, **134**, 13926-13929.
179. B. Yuan, Y. Pan, Y. Li, B. Yin and H. Jiang, *Angew. Chem. Int. Ed.*, 2010, **49**, 4054-4058.
180. J. Chen, R. Liu, Y. Guo, L. Chen and H. Gao, *ACS Catal.*, 2015, **5**, 722-733.

181.   V. Pascanu, F. Carson, M. V. Solano, J. Su, X. Zou, M. J. Johansson and B. Martin-Matute, *Chem. Eur. J.*, 2016, **22**, 3729-3737.

182.   J. D. Xiao, Q. Shang, Y. Xiong, Q. Zhang, Y. Luo, S. H. Yu and H. L. Jiang, *Angew. Chem. Int. Ed.*, 2016, **55**, 9389-9393.

183.   L. Chen, H. Chen, R. Luque and Y. Li, *Chem. Sci.*, 2014, **5**, 3708-3714.

184.   L. Chen, B. Huang, X. Qiu, X. Wang, R. Luque and Y. Li, *Chem. Sci.*, 2016, **7**, 228-233.

185.   X. H. Liu, J. G. Ma, Z. Niu, G. M. Yang and P. Cheng, *Angew. Chem. Int. Ed.*, 2015, **54**, 988-991.

186.   V. I. Isaeva, O. L. Eliseev, R. V. Kazantsev, V. V. Chernyshev, P. E. Davydov, B. R. Saifutdinov, A. L. Lapidus and L. M. Kustov, *Dalton Trans.*, 2016, **45**, 12006-12014.

187.   D. Wang, Y. Song, J. Cai, L. Wu and Z. Li, *New J. Chem.*, 2016, **40**, 9170-9175.

188.   S. Patra, T. H. Crespo, A. Permyakova, C. Sicard, C. Serre, A. Chausse, N. Steunou and L. Legrand, *J. Mater. Chem. B*, 2015, **3**, 8983-8992.

189.   C. J. Stephenson, J. T. Hupp and O. K. Farha, *Inorg. Chem.*, 2016, **55**, 1361-1363.

190.   B. An, J. Zhang, K. Cheng, P. Ji, C. Wang and W. Lin, *J. Am. Chem. Soc.*, 2017, **139**, 3834-3840.

191.   Q. Yang, W. Liu, B. Wang, W. Zhang, X. Zeng, C. Zhang, Y. Qin, X. Sun, T. Wu, J. Liu, F. Huo and J. Lu, *Nat. Commun.*, 2017, **8**, 14429.

192.   B. Wang, W. Liu, W. Zhang and J. Liu, *Nano Res.*, 2017, **10**, 3826-3835.

193.   B. Xiao, P. J. Byrne, P. S. Wheatley, D. S. Wragg, X. Zhao, A. J. Fletcher, K. M. Thomas, L. Peters, J. S. O. Evans, J. E. Warren, W. Zhou and R. E. Morris, *Nat. Chem.*, 2009, **1**, 289-294.

194.   S. Diring, D. O. Wang, C. Kim, M. Kondo, Y. Chen, S. Kitagawa, K. Kamei and S. Furukawa, *Nat. Commun.*, 2013, **4**, 2684.

195.   T. Lee, Z. X. Liu and H. L. Lee, *Cryst. Growth Des.*, 2011, **11**, 4146-4154.

196.   T. Lee, H. Lin Lee, M. Hsun Tsai, S. L. Cheng, S. W. Lee, J. C. Hu and L. T. Chen, *Biosens. Bioelectron.*, 2013, **43**, 56-62.

197.   W. Ma, Q. Jiang, P. Yu, L. Yang and L. Mao, *Anal. Chem.*, 2013, **85**, 7550-7557.

198.   J. W. Zhang, H. T. Zhang, Z. Y. Du, X. Wang, S. H. Yu and H. L. Jiang, *Chem. Commun.*, 2014, **50**, 1092-1094.

199.   K. Liang, R. Ricco, C. M. Doherty, M. J. Styles, S. Bell, N. Kirby, S. Mudie, D. Haylock, A. J. Hill, C. J. Doonan and P. Falcaro, *Nat. Commun.*, 2015, **6**, 7240.

200.   K. Liang, C. J. Coghlan, S. G. Bell, C. Doonan and P. Falcaro, *Chem. Commun.*, 2016, **52**, 473-476.

201.   K. Liang, R. Ricco, C. M. Doherty, M. J. Styles and P. Falcaro, *CrystEngComm*, 2016, **18**, 4264-4267.

202.   K. Liang, R. Wang, M. Boutter, C. M. Doherty, X. Mulet and J. J. Richardson, *Chem. Commun.*, 2017, **53**, 1249-1252.

203.   H. M. He, H. B. Han, H. Shi, Y. Y. Tian, F. X. Sun, Y. Song, Q. S. Li and G. S. Zhu, *ACS Appl. Mater. Interfaces*, 2016, **8**, 24517-24524.

204.   K. Liang, C. Carbonell, M. J. Styles, R. Ricco, J. Cui, J. J. Richardson, D. Maspoch, F. Caruso and P. Falcaro, *Adv. Mater.*, 2015, **27**, 7293-7298.

205.   S. B. Li, M. Dharmarwardana, R. P. Welch, Y. X. Ren, C. M. Thompson, R. A. Smaldone and J. J. Gassensmith, *Angew. Chem. Int. Ed.*, 2016, **55**, 10691-10696.